INVITED PAPER

Capacity Trends and Limits of Optical Communication Networks

Discussed in this paper are: optical communication network traffic evolution trends, required capacity and challenges to reaching it, and basic limits to capacity.

By René-Jean Essiambre, *Senior Member IEEE*, and Robert W. Tkach, *Fellow IEEE*

ABSTRACT | Since the first deployments of fiber-optic communication systems three decades ago, the capacity carried by a single-mode optical fiber has increased by a staggering 10 000 times. Most of the growth occurred in the first two decades with growth slowing to ten times in the last decade. Over the same three decades, network traffic has increased by a much smaller factor of 100, but with most of the growth occurring in the last few years, when data started dominating network traffic. At the current growth rate, the next factor of 100 in network traffic growth will occur within a decade. The large difference in growth rates between the delivered fiber capacity and the traffic demand is expected to create a capacity shortage within a decade. The first part of the paper recounts the history of traffic and capacity growth and extrapolations for the future. The second part looks into the technological challenges of growing the capacity of single-mode fibers by presenting a capacity limit estimate of standard and advanced single-mode optical fibers. The third part presents elementary capacity considerations for transmission over multiple transmission modes and how it compares to a single-mode transmission. Finally, the last part of the paper discusses fibers supporting multiple spatial modes, including multimode and multicore fibers, and the role of digital processing techniques. Spatial multiplexing in fibers is expected to enable system capacity growth to match traffic growth in the next decades.

KEYWORDS | Channel capacity; communication system traffic; fiber nonlinear optics; multiple-input–multiple-output (MIMO); optical fiber communication; optical networks

Manuscript received August 19, 2011; revised December 12, 2011; accepted December 22, 2011. Date of publication March 16, 2012; date of current version April 18, 2012.
The authors are with Bell Laboratories, Alcatel-Lucent, Holmdel, NJ 07733 USA (e-mail: rene.essiambre@alcatel-lucent.com; bob.tkach@alcatel-lucent.com).

Digital Object Identifier: 10.1109/JPROC.2012.2182970

I. INTRODUCTION

Optical communications is unchallenged for the transmission of large amounts of data over long distances with low latency and it underlies modern communications networks, in particular the internet. The transmission capacity of optical network technology has made dramatic strides over the decades since its introduction in the early 1970s. The early years of optical communications were characterized by a steady development of technology, a moderate rate of increase of bit rate in the single optical channel supported on these systems and the gradual change of the optical frequency transmission windows from 800 to 1300 to 1550 nm [1]–[3]. The latter part of the 1990s saw dramatic increases in system capacity brought about through the use of wavelength division multiplexing (WDM) enabled by optical amplifiers. This technological revolution ignited massive investment in system development both from traditional vendors as well as new entrants, and the capacity of commercial lightwave systems increased from less than 100 Mb/s when they debuted in the 1970s to roughly 1 Tb/s by 2000 [4]. This is an increase of more than 10 000 times in 30 years, but more incredibly, the introduction of WDM resulted in a factor of 1000 increase in just 10 years. This was enabled by the simple addition of more wavelengths to systems which were not limited by the available optical bandwidth. In the last decade, progress has slowed dramatically since the readily available bandwidth has become occupied and increases in capacity now require improvements in the efficiency of the utilization of optical bandwidth. The rapid growth in system capacity catalyzed by WDM resulted in system capacities that exceeded the requirements of network traffic for most of the past decade. However, the continued rapid growth of traffic has reversed this situation and now the need for increased system capacity is

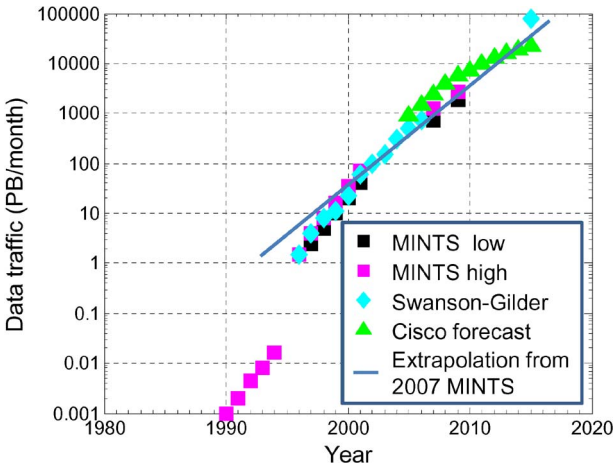

Fig. 1. ***North American Internet traffic.***

becoming acute. The current trends of traffic growth and system capacity increase will result in system capacity falling behind traffic by a factor of 10 over the next decade. Scaling system capacity to meet this challenge will be difficult and will require breakthroughs on a similar scale to the introduction of large-scale wavelength division multiplexing. This growth in traffic coupled with observed trends in commercial practice will also result in a requirement for interfaces to the core network to migrate from the current 10, 40, and 100 Gb/s to 1 Tb/s by 2020. Terabit single-channel bit rates seem extremely difficult to achieve by pursuing current technological paths.

In this paper, we present an overview of the challenges associated to the rapid growth of traffic demand and of the slower growth in network capacity. We evaluate a maximum fiber capacity estimate for a wide variety of single-mode fibers and discuss possible capacity scaling through spatial multiplexing in fibers and associated new fiber technologies.

II. NETWORK TRAFFIC

Internet traffic has been growing strongly since the earliest days of personal computers. At various times different applications have been cited as the drivers of this growth, but an examination of growth rates shows a fairly steady growth rate over the last 15 years [5].[1] Fig. 1 shows North American Internet traffic data from various sources over the period from 1990 through the present and some forecasts through 2015. There are two sources for the traffic data: the Minnesota Internet Traffic Study (MINTS) [6] and a report from the Discovery Institute by Swanson and Gilder [7]. The MINTS data shows a period of rapid growth in 1996, but the remainder of the years show a growth rate ranging from 100% a year in the early years to 50% to 60% a year since 2000. The latest growth rate estimate from this data is 50% to 60% a year as of year-end 2008. The Swanson and Gilder data shows very good agreement with the MINTS data. The other set of points on the chart are from a forecast prepared by Cisco in 2007 [8] and revised in 2011 [9]. The 2007 forecast is consistent with the 2008 data from MINTS and predicts a similar growth rate until 2011, while the 2011 revision suggests a slightly reduced growth rate. While the current estimated growth rates are far less than the "doubling every 100 days" sometimes quoted in the late 1990s through 2000 [10], they still give rise to an increase in traffic by a factor of 100 in 10 years. The solid line on Fig. 1 is set at the mean of the high and low estimates for 2007 and extrapolated using the estimated growth rate for year-end 2008. It is clear that the growth rate has been fairly consistent since 2000. While there are a variety of services that underlie the traffic demand described above it is possible to see a reason for the traffic growth that is independent of the individual services but instead considers trends in the technology used to support those services. In particular, it is useful to look at the evolution of microprocessor speed and data storage. The Top 500 organization charts the performance increase of the 500 fastest supercomputers and has shown an increase of 10 times in 4 years since the early 1990s [11]. Individual microprocessors have shown a similar improvement rate. Since the data traffic we are interested in originates and terminates on machines made up of these processors, it is unsurprising that the traffic scales at essentially the same rate. Alternatively traffic can be thought of as movement of data. The International Data Corporation (IDC) has estimated the total amount of stored data to increase by a factor of 10 in 5 years again essentially equal to the rate of traffic increase [12]. Both the speed of the devices connected to the network and the total amount of information stored are scaling at the same rate we observe for network traffic and these underlying trends show no sign of abating.

III. SYSTEM CAPACITY

Optical communications underwent a revolution in the 1990s as optical amplifiers and WDM enabled the information carried on a single fiber to move from a few gigabits per second to over one terabit per second. This rapid expansion of system capacity is visible in Fig. 2. The points on the figure are total capacities for a single fiber in laboratory/research demonstrations. Points are also distinguished by whether WDM is employed. Generally, only points which represent a new record of capacity are plotted. Various time periods exhibit relatively stable growth rates with relatively sharp demarcations between them. We see an initial rapid rise in capacity for single-channel time division multiplexing (TDM) demonstrations as researchers employed available microwave components

[1]Some of the material in this section and the next has been presented in an earlier form in [5] but is updated and expanded here.

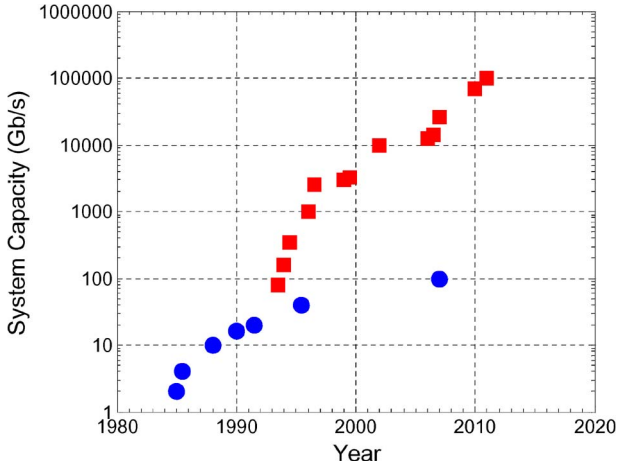

Fig. 2. ***Demonstrated system capacities. Single channel TDM systems (filled circles) WDM systems (filled squares).***

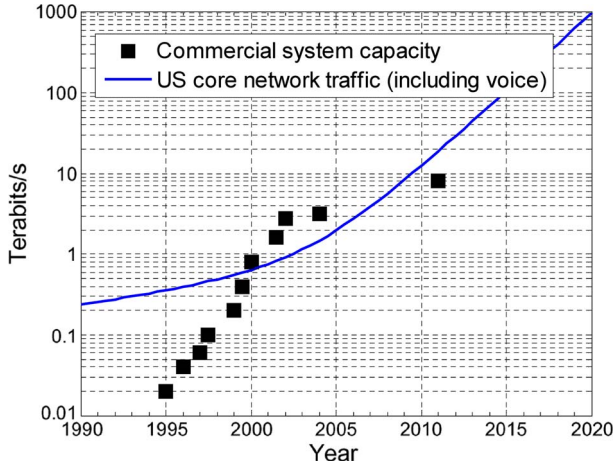

Fig. 4. ***Commercial system capacities (squares) and total network traffic including voice (blue curve) using measurements and projections from Fig. 1 and measured and projected voice traffic as of 1998.***

in digital circuits. Progress levels-off in the late 1980s as the optical system speed became limited by the speed of components and further progress was controlled by the rate of technological development of transistors. Another rapid rise in capacity begins in 1993 when the availability of optical amplifiers, dispersion management, and gain equalization enabled the application of WDM. The available spectrum was rapidly populated by more channels until 1996, when the spectrum was nearly filled, and the first 1 Tb/s experiments were being performed [13]–[15]. From this time until the present, a slower rate of capacity increase is observed as research focused on increased spectral efficiency (SE). Fig. 3 shows the SE achieved in these demonstrations as a function of year. It is clear from the figure that improvements in SE have driven the improvements in capacity. The current capacity record of 101.7 Tb/s achieved a SE of 11 b/s/Hz [16] (see Fig. 9) using coherent detection, offline processing and pilot-tone-based phase-noise mitigation. The modulation format is quadrature amplitude modulation (QAM) with 128 constellation points (128-QAM) [17]. The signal-to-noise ratio required for this format, combined with the limitations imposed by impairments arising from optical fiber nonlinearity, allowed transmission over only three relatively short, Raman-amplified spans. The SE of this result is impressive and it is worth noting that improving it by a factor of two via a more complex constellation would require the use of 16 384-QAM and would increase the required optical signal-to-noise ratio (OSNR) by about two orders of magnitude making transmission over useful distances impossible given the presence of nonlinear effects in fibers described in Section IV. Fig. 4 shows the capacity of commercial optical communication systems as a function of the year of introduction. These tend to track the research demonstrations of Fig. 3 with a three to seven year delay. The point at 8.8 Tb/s in late 2009 corresponds to a system with 88 100-Gb/s channels using polarization-multiplexed QPSK modulation and coherent detection. The solid lines in Fig. 4 provide a continuous representation of system capacity vs. year and are projected into the future. The slope of the line from 2000 forward corresponds to a growth rate of less than 20% per year. The curve in Fig. 4 is the composite network traffic composed of the data traffic extrapolation described above combined with voice traffic which dominated the network before 2002 but grows slowly. Notice that the total network traffic and system capacity cross twice. First, in 2000, commercial system capacity increases through the total network traffic and it became possible to buy a system that could carry the entire network traffic on a single fiber pair. Second, the

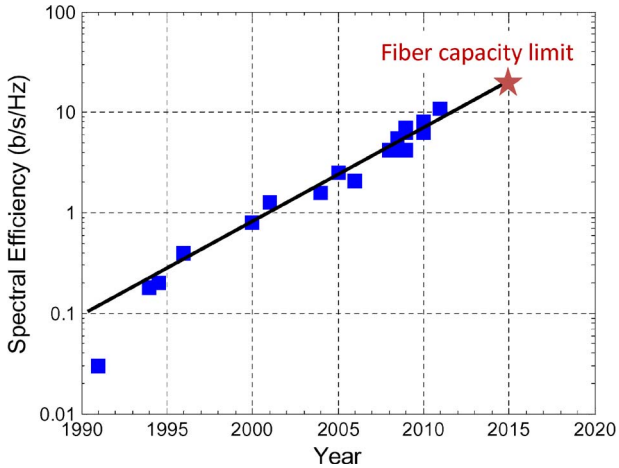

Fig. 3. ***Spectral efficiency achieved in research demonstrations versus year.***

two curves cross again in 2008, when traffic growth resulted in network traffic exceeding system capacity. In the following years the projected curves diverge with traffic outstripping capacity by more than a factor of 10 per decade.

It is important to note that there is no obvious reason to compare network traffic with the capacity of a single optical communication system; however, the comparison can be justified, at least when plotted on a logarithmic axis. The capacity of a link must obviously be larger than the traffic carried on that link; typically the factor is between two and five, accounting for peak to average traffic ratios [18]. Of course, the traffic on a link is not the same as the traffic in the network. In North America there are three to five links passing east to west, so we might expect that link traffic would be roughly three to five times lower than network traffic. These two errors are in opposing directions and one may hope that the comparison carries at least qualitative and order-of-magnitude value.

As system capacity scales to meet the growth of network traffic, it is important for the speed of interface rates to the networking equipment to increase as well in order to limit the increase in complexity of the network. Fig. 5 shows interface rates for a variety of networking equipment plotted against the year of commercial introduction. The plot starts with an early high-speed interface at 168 Mb/s [19], [20] through today. The years before 2000 are characterized by a variety of rates for various layers of the network, with cross connects and internet protocol (IP) routers using lower rates than those available for transmission. In 2000, we see a remarkable coalescing of rates at 10 Gb/s for transmission, cross connects, and routers. While this plot overstates the case, since interfaces introduced in earlier years persist in the network, it is clear that there has been a substantial flattening of the network; the utility of low bit rate circuits and the network elements that provision them becomes marginal as interface rates to nodal equipment rise. The line on the graph is drawn through the transmission points and attempts to project the evolution of interface rates into the next decade. This extrapolation suggests that 1-Tb/s interfaces will be used towards the end of the decade. The slope of the line is roughly a factor of 10 in 10 years—similar to that seen for the extrapolation of system capacity. Thus far we have only examined trends and extrapolated their continuation. Now we turn our attention to the requirements that these trends in traffic and capacity will place on system design. We begin by reviewing the evolution of some key system parameters. The earliest WDM systems had between four and eight 2.5-Gb/s channels and were introduced in 1995 [2]. These first systems had capacities on the order of 20 Gb/s and operated on a 200-GHz channel spacing resulting in a SE of 0.0125 b/s/Hz. By 2000, systems had rapidly advanced to 80 or more 10-Gb/s channels operating on 50-GHz spacing for capacities of nearly 1 Tb/s, and a SE of 0.2 b/s/Hz. Commercial systems introduced in 2010 operate with 100-Gb/s channels on 50-GHz spacing with SE of 2.0 b/s/Hz. To obtain the same factor of 10 improvement over the next decade would imply systems with 1-Tb/s channels, capacity of 100 Tb/s, and SE of 20 b/s/Hz. Clearly these are very challenging specifications. In fact, further increase in capacity will be hampered by significant limitations arising from fiber nonlinearity as we see below.

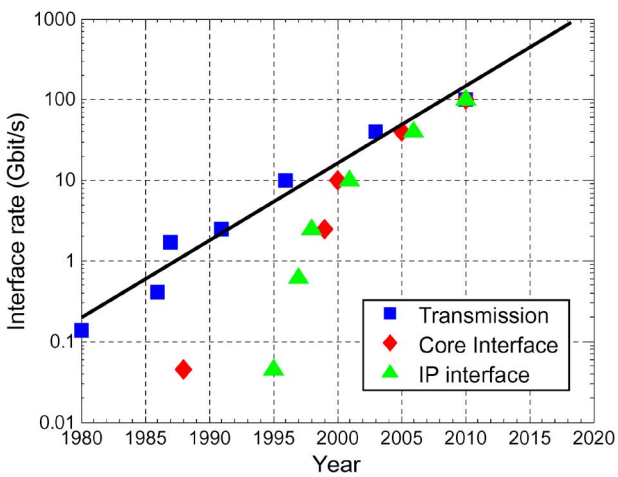

Fig. 5. ***Interface rates for a variety of networking equipment versus year of introduction. Optical communication systems (squares), cross connects (diamonds), and IP routers (triangles).***

IV. LIMITS TO SYSTEM CAPACITY

As shown in Fig. 2, there has been a tremendous increase in capacity of three orders of magnitude in the last two decades. Clearly, it is of interest to investigate whether there are fundamental limits to this capacity increase. In this section, we first briefly review Shannon's information theory for the additive white Gaussian noise (AWGN) channel and then present results of calculations of a "nonlinear Shannon limit" associated to the presence of the Kerr nonlinear effects in fibers.

A. Shannon Capacity

The notion of "capacity" of a channel was introduced in 1948 by Claude Shannon [22].[2] The capacity of a channel can be described as the asymptote of the rates of transmission of information that can be achieved with arbitrarily low error rate. In his seminal work [22], Shannon focused primarily on a channel that adds white Gaussian noise, and more specifically, the AWGN channel [23]–[25]. In the last 60 years, Shannon's "information

[2]A channel in the sense of Shannon is not to be confused with a WDM channel in optical communication, which is a signal occupying a certain frequency band, often contaminated by noise and other sources of distortion.

theory" has been applied and adapted to more complex channels such as wireless communication [26]–[33], digital subscriber lines (DSLs) over twisted copper wires [34]–[38], coaxial cables [36]–[39] and the "photon channel" [40]–[45], relevant to deep space and satellite communications [46], [47].

We review in this section the capacity relations for a *single-channel* with AWGN that we later use as a reference in the multiple channels Section V-A. For a bandlimited channel, it is convenient[3] to quote the SE defined as the capacity C per unit of bandwidth B. From Shannon's theory, the SE of a single AWGN channel is given by the well-known relation [23], [25]

$$\mathrm{SE} \equiv \frac{C}{B} = \log_2(1 + \mathrm{SNR}) \tag{1}$$

where the signal-to-noise ratio SNR is defined as $\mathrm{SNR} = P/N$ where P is the signal average power and N the noise average power in a bandwidth B. We consider here a signal constructed from a serial concatenation of symbols at a rate of R_s symbols per seconds. Many bits of information can be encoded using the amplitude and phase of the signal on each symbol. The minimum bandwidth that such a signal can have while remaining free from intersymbol interference (ISI) [48], [49] at the optimum sampling point is equal to the value of the symbol rate R_s [22], [50]–[52]. This signal is generated using a field waveform of the form $\sin(t)/t$ associated with each symbol [17], [48]. For such a minimum-bandwidth signal, the noise power $N = N_0 R_s$, where N_0 is the noise power spectral density. The SNR can be written as [30], [31], [48], [49]

$$\mathrm{SNR} \equiv \frac{P}{N} = \frac{P}{N_0 R_s} = \frac{E_s}{N_0} \tag{2}$$

where the last equality is obtained using the relation $P = E_s R_s$, where E_s is the energy per symbol. Note that both, signal and noise, are represented by complex fields, each having two quadratures. At low SNR, (1) can be approximated by

$$\mathrm{SE} \approx \frac{1}{\ln 2}\left(\mathrm{SNR} - \frac{\mathrm{SNR}^2}{2}\right). \tag{3}$$

[3]For simplicity, we use the word capacity to refer to either capacity or *SE* in this paper as both are simply related by the channel bandwidth B.

An interesting observation from (3) is that both SE and SNR, or E_s at fixed N_0, go to zero simultaneously, i.e., one cannot achieve high SE at low SNR on a single channel.

Using (2) one can define an SNR *per bit*, SNR_b, as [25], [48], [49]

$$\frac{E_b}{N_0} \equiv \mathrm{SNR}_b = \frac{\mathrm{SNR}}{\mathrm{SE}} \tag{4}$$

where the energy per bit $E_b = E_s/\mathrm{SE}$. The SNR per bit can therefore be interpreted as the energy per bit per unit of noise power spectral density. Equation (1) can be reexpressed as

$$\mathrm{SNR}_b = \frac{2^{\mathrm{SE}} - 1}{\mathrm{SE}}. \tag{5}$$

The SNR per bit can be written as $\mathrm{SNR}_b = E_b/N_0$ where $E_b = E_s/\mathrm{SE}$ is the energy per bit. At high SE, $\mathrm{SNR}_b \sim 2^{\mathrm{SE}}/\mathrm{SE}$.

One can write (5) as a series expansion around $\mathrm{SE} = 0$. It is given by $\mathrm{SNR}_b = \sum_{q=0}^{Q} (\ln 2)^{q+1} \mathrm{SE}^q/(q+1)!$. Expansion to second order and at low SE gives

$$\mathrm{SNR}_b \approx \ln 2 + \frac{(\ln 2)^2}{2}\mathrm{SE} + \frac{(\ln 2)^3}{6}\mathrm{SE}^2. \tag{6}$$

One notes that, in contrast to the relation between SE and SNR of (3), the SNR per bit, SNR_b, does not go to zero when SE goes to zero, but assumes a minimum value

$$\mathrm{SNR}_b^{\min} = \ln 2 \tag{7}$$

or ~ -1.59 dB [53] (see Fig. 6). There is, therefore, a minimum SNR or energy per bit to transmit information over the AWGN channel [23], [25] and this minimum occurs at low SNR.

It is interesting to define the ratio $\Delta\mathrm{SNR}_b$

$$\Delta\mathrm{SNR}_b \equiv \mathrm{SNR}_b/\mathrm{SNR}_b^{\min} \tag{8}$$

which can be referred to as an excess SNR or energy per bit at which a system operates. The quantity $\Delta\mathrm{SNR}_b$, in dB, is represented schematically on the Shannon curve of Fig. 6,

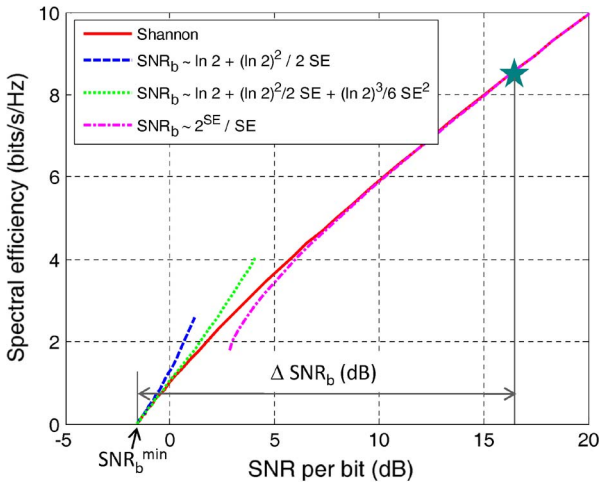

Fig. 6. ***Spectral efficiency versus SNR per bit for a single channel, a few approximations of SNR_b and a graphic representation of ΔSNR_b.***

which also shows the approximation to first and second order in SE from (6).

We can also express the SE as a function of SNR_b to first order in SNR_b as

$$\mathrm{SE} \approx \frac{2}{(\ln 2)^2}\left(\mathrm{SNR}_b - \mathrm{SNR}_b^{\min}\right). \tag{9}$$

B. Relations between SNR and OSNR

In optical communication, the *optical* signal-to-noise ratio is the quantity typically reported to characterize the ratio between signal and noise. In other areas of digital communication, the SNR is used. The quantities involved in both OSNR and SNR definitions are displayed in Fig. 7. The OSNR is written as

$$\mathrm{OSNR} = \frac{P}{2N_{\mathrm{ASE}}B_{\mathrm{ref}}} \tag{10}$$

where P is the average signal power, summed over the two states of polarization if polarization division multiplexing (PDM) is used, N_{ASE} is the spectral density of amplified spontaneous emission per polarization and B_{ref} is a reference bandwidth, commonly taken to be 0.1 nm, which corresponds to 12.5 GHz at 1550 nm. Note that the definition of OSNR does not require the signal to carry any data since the OSNR definition uses a *fixed* reference bandwidth B_{ref} instead of the symbol rate R_s used in the SNR definition [see (2)]. The OSNR also considers the noise in both polarization states independent of whether PDM of the signal is used or not. From (2) and (10), the relation between OSNR and SNR can be expressed as

$$\mathrm{OSNR} = \frac{pR_s}{2B_{\mathrm{ref}}}\mathrm{SNR} \tag{11}$$

where $p = 1$ for a singly-polarized signal and $p = 2$ for a PDM signal, and where N_{ASE} and N_0 have canceled each other out since they represent the same physical quantity, the noise power spectral density [17].

Equation (12) can also be written in the following form

$$\mathrm{OSNR} = \frac{R_s}{B_{\mathrm{ref}}}\mathrm{SNR}^{(2)} \tag{12}$$

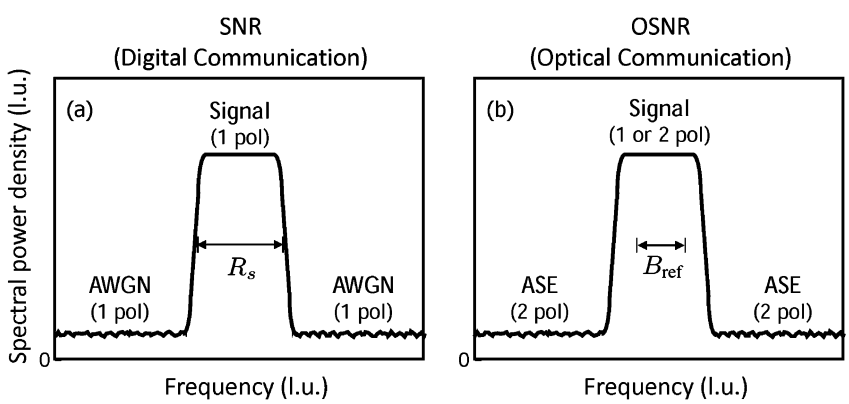

Fig. 7. ***Definition of signal and noise for the (a) signal-to-noise ratio (SNR) and (b) optical signal-to-noise ratio (OSNR). l.u.: linear units.***

where $\mathrm{SNR}^{(2)}$ is the average SNR over the two polarization modes. It is defined as

$$\mathrm{SNR}^{(2)} \equiv \frac{P_x + P_y}{N_x + N_y} \tag{13}$$

where the indices x and y refer to the x and y polarizations, respectively. In this definition of $\mathrm{SNR}^{(2)}$, when the signal is singly-polarized, the signal power originates from one polarization while the noise power remains summed over both polarizations. This definition of SNR has the advantage that it can easily be generalized to a large number of modes [see (21)].

We define the information bit rate $R_b^{(p)}$, in bits per second, as the sum of the information rates in both polarization states. Assuming the same structure of the signal for both polarizations if PDM is used, i.e., same symbol rate R_s, same number of constellation points per polarization $\mathcal{M}$, and same code rate $\tilde{R}_c$, the bit rate $R_b^{(p)}$, valid for a singly-polarized or a PDM signal, can be written as

$$R_b^{(p)} = p\tilde{R}_c \log_2(\mathcal{M}) R_s \tag{14}$$

where $\tilde{R}_c$ is the encoder rate, which represents the ratio of input to output bits at the encoder so that $0 < \tilde{R}_c \leq 1$. Note that the transmission information rate in bits per symbol $\tilde{R} = \tilde{R}_c \log_2(\mathcal{M})$ can be identified to the SE in Shannon's formula (1) for an ideal code and a Gaussian constellation. For PDM, a symbol corresponding to the symbol rate R_s extends to both polarization states and represents all the possible ways to combine the $\mathcal{M}$ symbol(s) of each polarization. The symbol size at the symbol rate R_s is therefore $\mathcal{M}^p$ with $p = 2$. One can see that (14) can be written in a more natural form as $R_b^{(p)} = \tilde{R}_c \log_2(\mathcal{M}^p) R_s$, where $\log_2(\mathcal{M}^p)$ represents the number of uncoded bits of the constellation at R_s. Using (4), one can express (12) as

$$\mathrm{OSNR} = \frac{R_b^{(p)}}{2B_{\mathrm{ref}}} \mathrm{SNR}_b \tag{15}$$

where SNR_b is the SNR per bit in one of the polarization state having a signal.

Note that the relation between OSNR and SNR_b requires only the knowledge of $R_b^{(p)}$, but does not require to know whether the signal is singly-polarized or if PDM is used. Equation (15) can be also expressed as

$$\mathrm{OSNR} = \frac{R_b^{(p)}}{pB_{\mathrm{ref}}} \mathrm{SNR}_b^{(2)} \tag{16}$$

where $\mathrm{SNR}_b^{(2)} = p\mathrm{SNR}_b/2$ is the SNR per bit accounting for the two polarization modes.

C. Nonlinear Shannon Limit for a Nonlinear Fiber Channel

It is only relatively recently that information theoretic approaches have been applied to fiber-optic communication systems based on single-mode fibers (SMFs) [17], [54]–[79] (more details can be found in [17]). This 'late' focus on the "fiber channel" is mainly due to the fact that an optical fiber is a *Kerr nonlinear medium* [80]–[83], which raises many challenges. One of them is that there is no well established framework of information theory to calculate the capacity of a channel that is simultaneously nonlinear and bandwidth-limited. A second difficulty is the absence of closed-form analytic expressions describing fiber propagation for arbitrary input signal shapes and power levels.

Capacity limitations of the most commonly studied channels originate from the presence of in-band sources of distortion, being either in-band noise or some form of in-band interference coming from other sources [30], [31], [84]. The capacity of these channels typically increases monotonically with power. In the case of the nonlinear fiber channel, the capacity is limited by noise at low power but becomes limited by fiber nonlinearity as power increases. Remarkably, in the context of optically-routed networks (ORNs), the high-power fiber capacity limitations originate mainly from fields present outside the bandwidth of the signal of interest [17] and lead to a *maximum capacity*. Fig. 8 illustrates schematically the nonlinear process that results in capacity limitation for the nonlinear fiber channel. The presence in a fiber of a WDM channel occupying a distinct frequency band from a WDM channel of interest, changes the refractive index of the fiber medium through the Kerr nonlinear effect [85]. Since

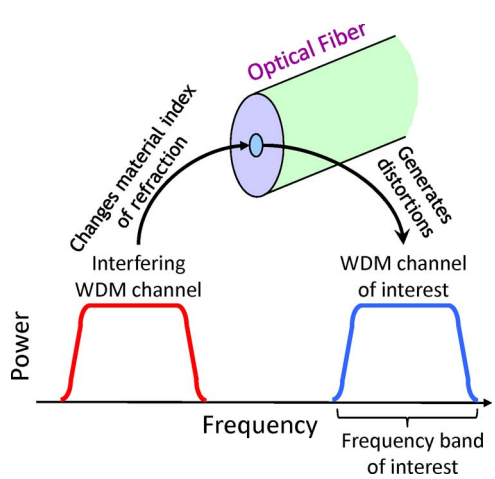

Fig. 8. ***Schematic illustration of the main nonlinear process limiting capacity in fiber.***

Table 1 Assumptions in the Model to Calculate a Fiber Capacity Estimate

Modulation	Raised-cosine spectrum
Constellation	Equally-spaced rings
Coding	Calculate the mutual information
Optical amplification	Ideal distributed Raman
Optical filtering	Periodic ideal square filters at ROADMs
Receiver	Ideal coherent detection
Digital signal processing	Reverse nonlinear propagation
Optical networking	Out-of-band fields assumed unknown

the WDM channel of interest is also present in the fiber, it experiences these variations of refractive index and becomes distorted. In general, the change of refractive index depends not only on power but also on the *data* being transmitted [86]–[88]. Since different WDM frequency bands are optically routed to different physical locations in optical networks, the data of the copropagating WDM channels are not known and distortions created by copropagating WDM channels on the WDM channel of interest cannot be fully compensated [17].

Nonlinear propagation through optical fibers is described by the partial differential equation [17]

$$\frac{\partial E}{\partial z} + \frac{i}{2}\beta_2 \frac{\partial^2 E}{\partial t^2} - i\gamma |E|^2 E = i\mathcal{N} \tag{17}$$

where $E(z,t)$ is the optical field at a given location z and time t, β_2 is the fiber chromatic dispersion, γ the fiber nonlinear coefficient and $\mathcal{N}(z,t)$ is the field that represents amplified spontaneous emission (ASE). The field $E(z,t)$ is assumed to be singly polarized and (17) is written for a system using ideal distributed Raman amplification where the Raman gain continuously compensates for fiber loss [89]. The fiber nonlinear coefficient $\gamma = n_2\omega_s/(cA_{\text{eff}})$ where n_2 is the fiber nonlinear refractive index [83], $\omega_s = 2\pi\nu_s$ is the angular optical frequency at the signal wavelength with ν_s being the optical carrier frequency, c the speed of light and A_{eff} the fiber effective area [83].

Assuming that ASE generated by optical amplification can be represented by an AWGN source [90], [91], Shannon's information theory can therefore be applied to evaluate the impact of ASE noise on capacity. The autocorrelation [92] of the ASE field $\mathcal{N}(z,t)$ is given by [93]–[95]

$$\mathcal{E}[\mathcal{N}(z,t)\mathcal{N}^*(z',t')] = \alpha L h \nu_s K_T \delta(z-z')\delta(t-t') \tag{18}$$

where $\mathcal{E}[\cdot]$ is the expectation value operator and δ the Dirac functional. The factor $K_T = 1 + \eta(T,\nu_s,\nu_p)$ where $\eta(T,\nu_s,\nu_p)$ is the phonon occupancy factor [17], [96], [97]. The value of $K_T \sim 1.13$ at room temperature.

For ideal distributed Raman amplification, the noise spectral density per state of polarization can be written as [53], [89]

$$N_{\text{ASE}} = \alpha L h \nu_s K_T \tag{19}$$

where L is the system length and h the Planck constant. The noise power per polarization is simply $N_{\text{ASE}}R_s$.

The capacity calculation of the nonlinear fiber channel in the context of ORNs has been performed under certain assumptions summarized in Table 1. Fiber capacities are computed for a single WDM channel of interest in an ORN, assuming that all other WDM channels are simultaneously present, but not known at the transmitter or receiver. The constellations adopted are concentric ring constellations that approach closely the Shannon capacity even though a small gap from Shannon curves that can be seen at SNR $\lesssim$ 25 dB in Fig. 9 still remains. Routing in the network is performed using optical filters approaching the ideal square shape and is performed sufficiently frequently (every 100 km) that more frequent use of optical filters does not impact capacity. The signal is recovered by first performing ideal coherent detection followed by digital signal processing using reverse

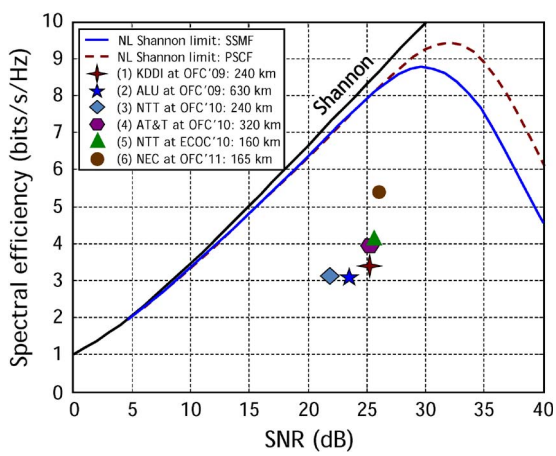

Fig. 9. ***Nonlinear capacity limit for transmission over 500 km of SSMF and PSCF and current record capacity experiments. The SSMF parameters are given in Table 2 and PSCF in the main text. The experiments (1)–(6) are from [98]–[102] and [16], respectively.***

Table 2 Standard Single-Mode Fiber Parameters

Dispersion D	17 ps/(nm-km)
Dispersion slope	Set to zero
Loss coefficient α_{dB}	0.2 dB/km
Nonlinear refractive index n_2	2.5×10^{-20} m^2/W
Effective area A_{eff}	80 μm^2
Nonlinear coefficient γ	1.27 (W-km)$^{-1}$
Wavelength λ	1550 nm
Optical frequency ν_s	193.41 THz

nonlinear propagation performed on the fields present in the frequency band of the WDM channel of interest. Because of the various approximations made during the evaluation of capacity, we refer to these nonlinear fiber capacities as estimates. Extensive explanations on how the nonlinear fiber capacity calculations have been performed can be found in [17], [70].

D. Standard Single-Mode Fiber

The parameters of the standard single-mode fiber (SSMF) are given in Table 2 and the corresponding nonlinear capacity estimate is given in Fig. 9. The six filled symbols in Fig. 9 represent the latest record SE experiments (from 2009 to August 2011) that propagate over at least 100 km. Also shown are the calculated nonlinear capacity estimates when the loss coefficient $\alpha =$ 0.15 dB/km and the effective area $A_{\text{eff}} = 120$ μm^2, parameters achievable for pure silica-core fibers (PSCFs). The experimental results are within a factor 1.6 to 3 from the estimated capacity. Note that the highest SE experiments have been achieved for distances shorter than 500 km and that a reduction in SE is expected if the distance were to be extended to 500 km.

Calculations of nonlinear fiber capacity estimates have been performed for various distances and the results are displayed in Fig. 10. One observes that the SNR at which the capacity peaks decreases by ~2.65 dB for every doubling of the distance. Since the ASE noise power increases by 3 dB when the distance doubles, the optimum signal power has a weak dependence on distance, decreasing by only 1.4 dB for the range of distance of 500 to 8000 km. One can understand this surprising result by realizing that higher capacities are achieved using denser constellations (larger $\mathcal{M}$), and that the larger the constellation, the more sensitive a signal is to nonlinear distortions. These larger constellations prevent raising the signal power significantly, even when the transmission distance is shortened dramatically. Note that having a nearly distance-independent optimum signal power is advantageous in network designs, since optical amplifiers can operate at nearly the same power per WDM channel for a wide range of distances.

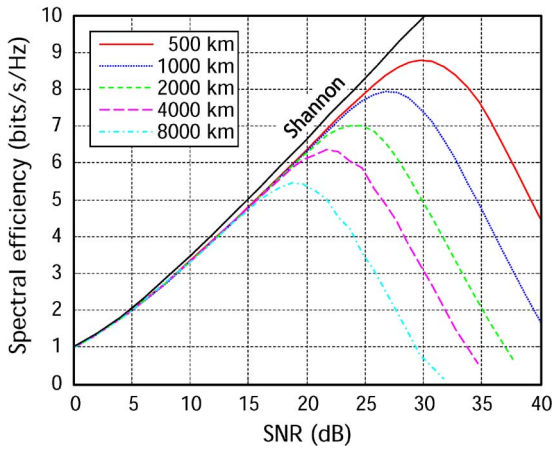

Fig. 10. ***Nonlinear capacity curves for a range of transmission distances.***

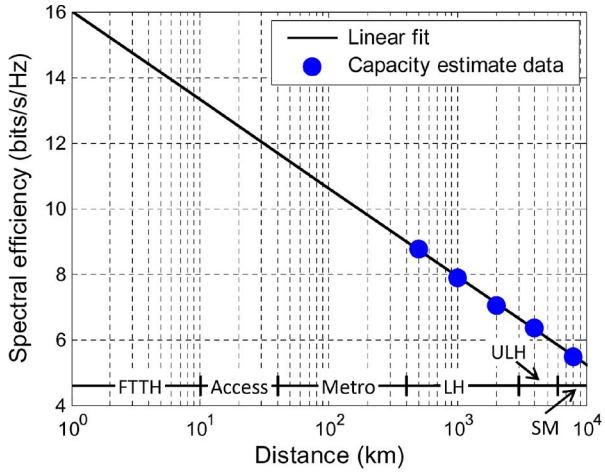

Fig. 11. ***Spectral efficiency as a function of distance from data at maximum capacity of Fig. 10. A linear fit to the data is also provided along with the type of networks it can be applied to.***

Fig. 11 shows the maximum SE values for each curve in Fig. 10. These calculated SE values fit well a linear relation when the distance is plotted in a logarithmic scale, so a linear fit to the SE is also shown in Fig. 11.

The types of networks covered by the various distances of the plot are shown near the bottom. As can be seen in the figure, the maximum SE of submarine (SM), ultra-long-haul (ULH), and long-haul (LH) does not vary widely considering that the range of distances covered is more than one order of magnitude. The maximum SE increases as the distance decreases to metropolitan (metro) and access networks. Finally, fiber-to-the-home (FTTH) has the highest maximum SE, but, remarkably, only 3 times the maximum SE of SM systems. This is a rather small increase in maximum SE considering that there is a difference of four orders of magnitude in distance between these two types of networks. This illustrates the difficulty of increasing SE in optical networks based on SMFs.

E. Advanced Single-Mode Fibers

For a given optical networking scenario and optical amplification scheme, the nonlinear fiber capacity depends mainly on the fiber parameters and system length. We show below the calculated maximum nonlinear fiber capacity estimates when varying three fiber parameters: the fiber loss coefficient α, the fiber nonlinear coefficient γ, and fiber dispersion D.

1) Fiber Loss: Fig. 12 shows the dependence of the maximum nonlinear fiber capacity on the fiber loss coefficient α_{dB}, which relates to α of (17) by $\alpha_{\mathrm{dB}} = 10\ \log_{10}(e)\alpha$. One observes that the maximum nonlinear capacity does not increase dramatically with a large reduction of α_{dB}. For instance, reducing α_{dB} from 0.2 to 0.05 dB/km increases capacity only from ~8 to ~9 b/s/Hz. It is worth pointing out, however, that a decrease in fiber loss coefficient, which generally occurs at all wavelengths simultaneously, benefits greatly practical system deployments by either increasing the distance between amplification sites or by reducing the Raman pump power requirements.

It is interesting to note that the dependence of the maximum capacity on the fiber loss coefficient is nearly linear when α_{dB} is plotted on a log scale as seen in Fig. 12. Shown on the graph are SSMF typical fiber loss coefficient, the lowest fiber loss coefficient of 0.1484 dB/km achieved using PSCF [103], and conjectured 0.05 dB/km that may possibly be achievable for a hollow-core fiber (HCF) operating at 2 μm [104]. One can see in Fig. 12 that even though it represents a tremendous challenge to reduce the fiber loss coefficient below 0.15 dB/km, the benefit on capacity is surprisingly limited.

It is worth pointing out that the benefit of reducing the fiber loss coefficient will increase for systems not using ideal distributed Raman amplification, and especially for systems using discrete amplification based on erbium-doped fiber amplifiers (EDFAs) [105], [106]. The reason is that, in ideal distributed Raman amplification systems, the quantity of noise at the end of the system is proportional to α, while it is approximately proportional to $\exp(\alpha)$ in systems based on EDFAs [17, eq. (54)].

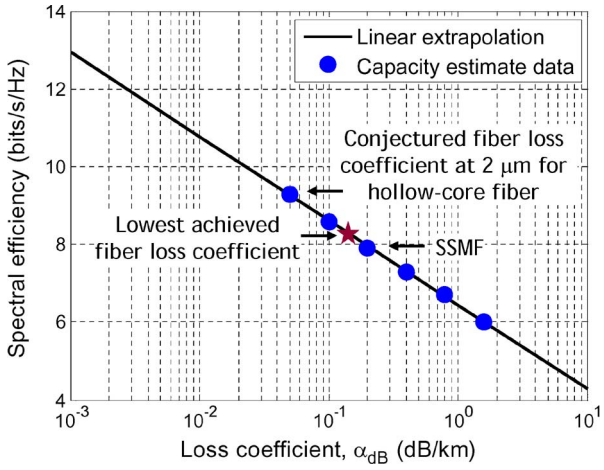

Fig. 12. ***Calculated maximum spectral efficiency for various fiber loss coefficients and a linear extrapolation.*** *L = **1000 km**, γ = **1.27** $(\mathbf{W\text{-}km})^{-1}$, and D = **17 ps**/(**nm-km**).*

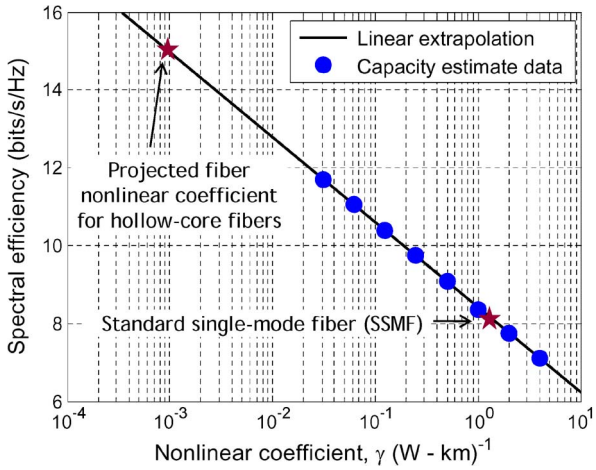

Fig. 13. ***Calculated maximum spectral efficiency for various fiber nonlinear coefficients and a linear extrapolation.*** *L = **500 km**, α_{dB} = **0.15 dB/km**, and D = **17 ps**/(**nm-km**).*

2) Fiber Nonlinear Coefficient: The fiber nonlinear coefficient can be made to vary by a change of the fiber material itself, material properties or through advances in fiber designs. The impact of varying the nonlinear coefficient γ on the maximum nonlinear fiber capacity is shown in Fig. 13 along with a linear extrapolation. A reduction of the fiber nonlinear coefficient has a similar effect on capacity as a reduction in the fiber loss coefficient. It is interesting to note that a reduction in the nonlinear coefficient by a factor of 1000, such as what can be nearly achieved by using HCFs [107], [108], would lead to an increase in capacity by only ~30%. Clearly, capacity scales very slowly with the nonlinear coefficient γ. Because they operate at lower SE due to higher noise levels, the impact of a reduction of γ has a higher relative impact on capacity in systems based on discrete EDFAs than for systems based on ideal distributed Raman amplification. However, for both system types, very large changes in γ are necessary to significantly increase capacity.

3) Fiber Dispersion: Fig. 14 shows the impact of varying the fiber chromatic dispersion D on maximum nonlinear fiber capacity. The relation between D and β_2 of (17) at a given wavelength λ is $D = -2\pi c\beta_2/\lambda^2$ [83]. The range of dispersion simulated covers the most common commercial fibers. A smaller variation of the maximum nonlinear fiber capacity is observed for dispersion than for the loss and

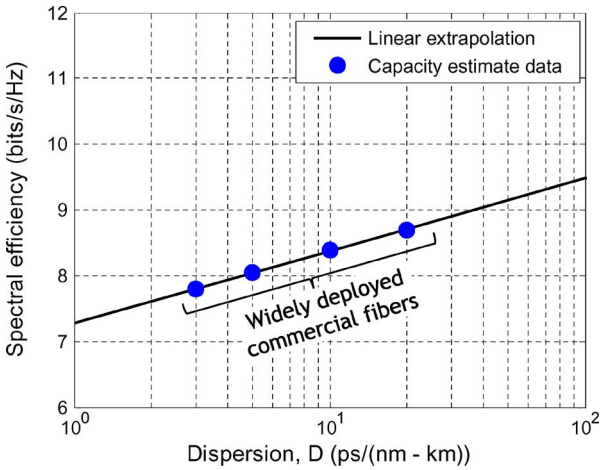

Fig. 14. ***Calculated maximum spectral efficiency for various fiber dispersion and a linear extrapolation.*** $L = 500$ ***km***, $\alpha_{dB} = 0.2$ ***dB/km***, $\gamma = 1.27$ $(\mathbf{W\text{-}km})^{-1}$.

nonlinear coefficients. These results suggest that, in proportion, a variation of chromatic dispersion has a lower impact on capacity than the two other fiber parameters considered.

V. SPATIAL MULTIPLEXING IN FIBERS

The cladding diameter of SMFs has been standardized in the 1970s to 125 μm. This diameter was chosen to be sufficiently large so that the fiber has sufficient strength and flexibility. The radial distribution of the spatial mode in SSMF can be approximated by a Gaussian of the form $E(r) = \exp(r^2/w^2)$ where r is the distance to the core center and $2w$ the mode field diameter [109], [110]. A typical value of $2w$ for SSMF is 10.4 μm. This gives a ratio between the field at the fiber center $(r = 0)$ to the field at the cladding outer interface $(r = 125\ \mu\text{m})$ of $\sim 10^{-63}$. Such an extraordinary low number is evidence of the low occupation of the fiber volume by the spatial mode of SSMF. Taking also into consideration the increase in mode confinement that can be achieved through advanced fiber index profile designs [111], it strongly suggests that many spatial modes with negligible overlap between parallel spatial modes could be supported within the same fiber volume. Such spatially separated modes make it easier to perform spatial multiplexing and demultiplexing [112]. To achieve a greater density of spatial modes, one can lift the requirement of low overlap between modes and use spatial filters to multiplex and demultiplex the spatial modes. In either case of low or large overlap between spatial modes, imperfection in waveguides structures, local changes in the material properties, fiber bending and twisting can couple the modes together. Fortunately, with the development of MIMO technologies [26], [27], [31], [115], it has become possible to disentangle coupled spatial modes and recover the data through processing. This opens the possibility of fiber with an even larger number of spatial modes, by allowing large coupling between modes to occur.

A. Shannon Capacity for Independent Channels

Let's now consider how transmission over M channels (in the sense of Shannon) compares to the single-channel transmission of Section IV-A in terms of SE [26], [27], [30], [31], [116]–[121] and energy per bit [30], [31], [118]–[127]. A channel here can be identified, for instance, with one of the two polarization modes in a SMF or one of many fiber spatial modes, or both spatial and polarization modes.

For the case of M modes, the bit rate $R_b^{(M)}$ is defined as the sum over all modes and can be simply written as

$$R_b^{(M)} = M\tilde{R}_c \log_2(\mathcal{M}) R_s \tag{20}$$

where M is the number of modes and $\tilde{R}_c$ and $\mathcal{M}$ are as defined before (14). For a fiber that supports p polarization modes and s spatial modes, the number of modes $M = p \times s$.

We consider in this section the elementary case of M independent parallel channels to help estimate the potential benefits of spatial multiplexing in fibers (see Section V-C) relative to single-mode case described in Section IV-A. The signal and noise powers in the mth channel are denoted by P_m and N_m, respectively. The *total* signal power in all channels is $P^{(M)} = \sum_{m=1}^{M} P_m$. The SNR in each channel m is $\text{SNR}_m = P_m/N_m$ and the average SNR is given by

$$\text{SNR}^{(M)} \equiv \frac{\sum_{m=1}^{M} P_m}{\sum_{m=1}^{M} N_m}. \tag{21}$$

Since (1) applies to each channel individually for independent channels, the SE of each channel, SE_m, can be written as

$$\text{SE}_m = \log_2(1 + \text{SNR}_m). \tag{22}$$

For M independent channels, the total SE, $\text{SE}^{(M)}$, is simply given by

$$\text{SE}^{(M)} = \sum_{m=1}^{M} \text{SE}_m = \sum_{m=1}^{M} \log_2(1 + \text{SNR}_m). \tag{23}$$

Interesting relations can be obtained when $\mathrm{SNR}_m \ll 1$ for all the M channels, where $\mathrm{SE}^{(M)}$ in (23) simplifies to

$$\mathrm{SE}^{(M)} \approx \frac{1}{\ln 2}\sum_{m=1}^{M}\mathrm{SNR}_m = \frac{1}{\ln 2}\sum_{m=1}^{M}\frac{P_m}{N_m}. \tag{24}$$

If we further assume that the noise present in all channels is identical to the noise produced in the reference single channel, which is a realistic first-order approximation for spatial multiplexing in fibers, i.e., $N_m = N$ for all values of m, $\mathrm{SE}^{(M)}$ simplifies to

$$\mathrm{SE}^{(M)} \approx \frac{1}{\ln 2}\sum_{m=1}^{M}\frac{P_m}{N} = \frac{P^{(M)}}{N\ln 2}. \tag{25}$$

Note that, in this regime of low SNR per channel, SE depends, to first order, only on the total signal power and not on the exact distribution of powers between channels.

Let's now consider systems for which all M channels have the same SNR_m that is not necessarily small: the total SE of the M channels, $\mathrm{SE}^{(M)}$, is simply M times the SE of each channel. If further, the signal powers in each of the M channels identical, i.e., $P_m = P_c$ and similarly all the noise powers are equal, i.e., $N_m = N$, $\mathrm{SE}^{(M)}$ can be written simply as

$$\mathrm{SE}^{(M)} = M\log_2\left(1+\frac{P_c}{N}\right) \tag{26}$$

$$= M\log_2(1+\rho\mathrm{SNR}) \tag{27}$$

where $\mathrm{SNR} = P/N$ is the SNR in the reference single channel and ρ is the ratio of the power in each channel P_c to P. The reason to express $\mathrm{SE}^{(M)}$ in terms of the ratio P_c/P is that, in fibers, P_c and P have maximum values determined by fiber nonlinearity and fiber types. In the limit of an infinite number of channels M with a fixed $P_c = P/M$, $\mathrm{SE}^{(\infty)} \to \mathrm{SNR}/\ln 2$, identical to the single-channel result of (3) to first order in SNR.

It is interesting to evaluate the gain in SE

$$G_{\mathrm{SE}} \equiv \frac{\mathrm{SE}^{(M)}}{\mathrm{SE}} \tag{28}$$

for various values of SNR and signal powers. Restricting ourselves to channels with identical noise per channel $N_m = N$ and identical signal power P_c in all channels, one can write G_{SE} as

$$G_{\mathrm{SE}} = \frac{M\log_2(1+\rho\mathrm{SNR})}{\log_2(1+\mathrm{SNR})}. \tag{29}$$

From (29), one can see that three independent parameters affect G_{SE}: the number of channels M, the ratio of powers $\rho = P_c/P$ and the SNR of the reference channel P/N. From (29), when the power per channel P_c equals the single-channel power P, $G_{\mathrm{SE}} = M$, as it should be for M independent channels. Also, when both $P_c \ll N$ and $P \ll N$, $G_{\mathrm{SE}} \approx MP_c/P$, i.e., the SE increases approximately by the ratio P_c/P above the value of M when the signal powers are below the noise power. The power per mode P_c that can be used for spatial multiplexing in fibers will depend on fiber nonlinearity and the design of the fiber used for spatial multiplexing (see Section V-C).

Fig. 15 plots the gain in SE, G_{SE}, in dB, as a function of the reference channel SNR for the case when the reference signal power P is divided equally between all M modes, i.e., $P_c = P/M$. Fig. 16 plots the same gain in SE but as a function of the SNR per bit. Note that for a given SNR, the maximum gain achievable is nearly reached for a given number of channels M_{split}, which value can be approximated simply by $M_{\mathrm{split}} \sim \lfloor \mathrm{SNR}_b \rfloor$. Any additional increase in the number of channels beyond M_{split} does not bring significant gain in SE for this type of power split. At high SNR or SNR per bit, G_{SE} tends asymptotically towards $10\log_{10} M$ (in dB) as expected.

Let's now consider the impact of the ratio of the power per channel P_c to the single-channel power P on the gain

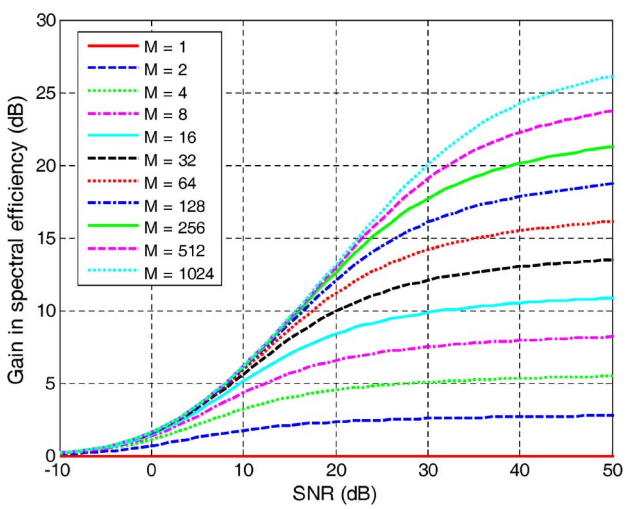

Fig. 15. *Gain in spectral efficiency G_{SE}, as a function of SNR of a single channel when the power P of a single channel is equally split between M independent channels.*

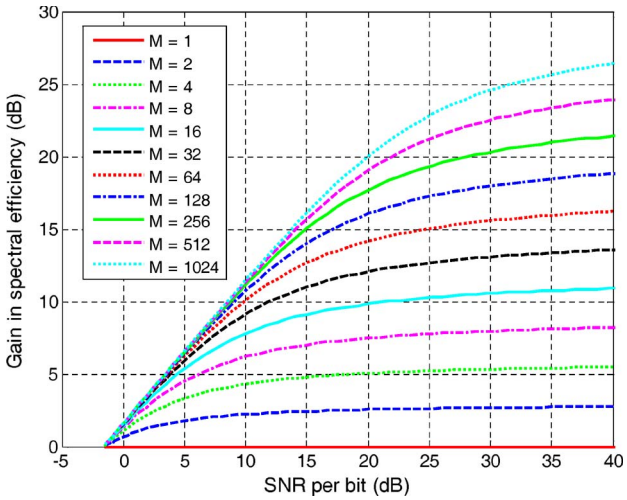

Fig. 16. *Same as Fig. 15 but as a function of SNR per bit.*

in SE. The ratio P_c/P is a relevant quantity that will be determined by the nonlinear effects present in fibers supporting multiple spatial modes. The impact on transmission of the various nonlinear effects is expected to depend greatly on fiber designs. From (29), one can see that the gain in SE per mode, G_{SE}/M, is a quantity independent of M. Fig. 17 shows the gain in SE per mode as a function of the ratio P_c/P for various values of SNR. A negative gain means a reduction in SE. As seen in Fig. 17, the highest values of SNR are the least affected by a reduction or increase in signal power per channel P_c relative to the single channel power P. This can be understood by the fact that a reduction of a few dBs in power when operating at high SNR on the SE curve changes the SE by only a small amount relative to the original SE, thereby producing lower gain or loss in SE. Note that this behavior is valid for an arbitrary number of channels M and that the curves for the gain in SE alone, G_{SE}, are identical to the curves in Fig. 17 but shifted up by $10\log_{10} M$. The maximum relative impact or reduced power per channel is therefore for systems operating at low SNR.

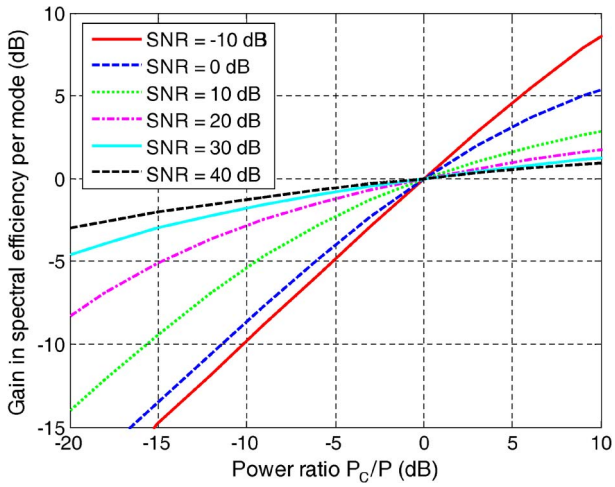

Fig. 17. *Gain in spectral efficiency per mode, G_{SE}/M, as a function of the ratio of the signal power per mode P_c to the single channel power P. These curves are independent of the number of modes M.*

A second quantity of interest is the gain in energy per bit, G_{E}, obtained by using M channels instead of a single channel to achieve a *fixed* SE [30], [31], [118], [123]–[126]. This gain G_{E} is defined as

$$G_{\mathrm{E}} \equiv \frac{\mathrm{SNR}_b}{\mathrm{SNR}_b^{(M)}} \tag{30}$$

where the SNR per bit for M modes, $\mathrm{SNR}_b^{(M)}$, is defined as

$$\mathrm{SNR}_b^{(M)} \equiv \left(\frac{E_b}{N_0}\right)^{(M)} = \frac{P^{(M)}}{\sum_m N_m}\frac{M}{\mathrm{SE}^{(M)}}. \tag{31}$$

This gain G_{E} is defined in such a way that a positive value of G_{E} corresponds to a system benefit, a reduction in energy per bit. One can express $\mathrm{SNR}_b^{(M)}$ in terms of the SE as

$$\mathrm{SNR}_b^{(M)} \equiv \frac{2^{\mathrm{SE}/M}-1}{\mathrm{SE}/M} \tag{32}$$

which, with the help of (5), gives for the gain in energy per bit in terms of SE as

$$G_{\mathrm{E}} = \frac{2^{\mathrm{SE}}-1}{M[2^{\mathrm{SE}/M}-1]}. \tag{33}$$

Fig. 18 shows G_{E} as a function of SE for various numbers of channels. A noticeable feature of G_{E} is that only a relatively small number of channels M is sufficient to obtain most of the gain in energy per bit. Increasing M beyond 16 barely increases G_{E} for the range of SEs displayed in Fig. 18. A simple equal split of signal power between two channels brings a large contribution to the power saving when using multiple channels.

It is interesting to note that the value of $\mathrm{SNR}_b^{(M)}$ is equal to the value of SNR_b of a single channel having a SE of SE/M. In the limit of infinite M, $\mathrm{SNR}_b^{(M)} = \ln 2 = \mathrm{SNR}_b^{\min}$ and $G_{\mathrm{E}} = \mathrm{SNR}_b/\mathrm{SNR}_b^{\min}$, which is the excess SNR per bit $\Delta\mathrm{SNR}_b$ defined in (8) for a single channel. Therefore, the

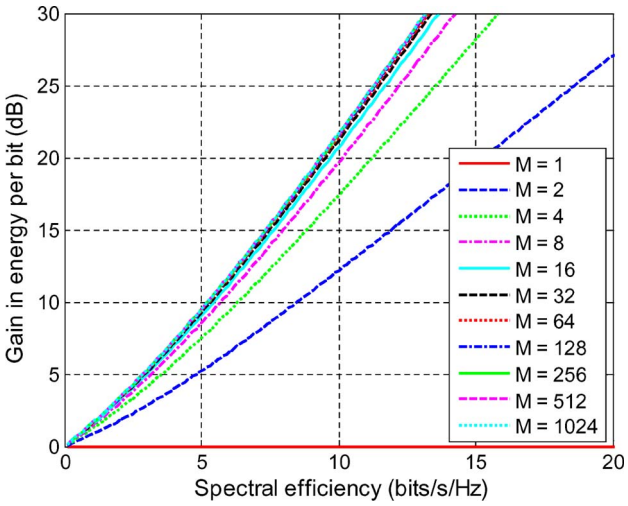

Fig. 18. ***Gain in energy per bit G_E obtained by using M channels compared to a single channel at identical SE. The power is equally split between the M channels.***

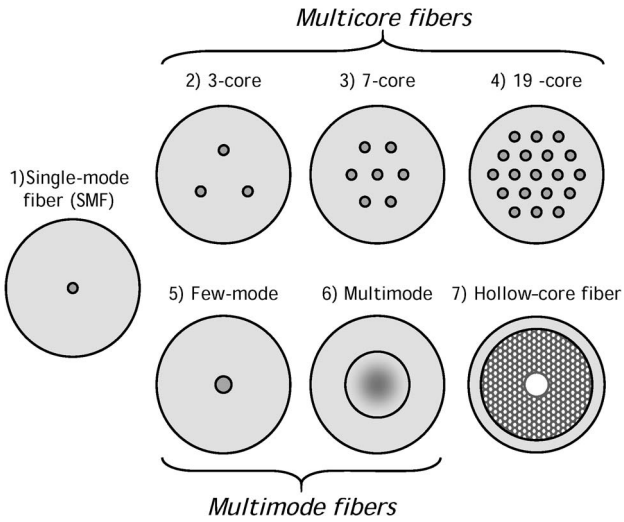

Fig. 20. ***Cross sections of a single-mode fiber and fibers supporting spatial multiplexing. Filled areas with darker shades of gray have a higher index of refraction (solid lines are shown as delimiters only).***

maximum energy saving from splitting a signal power equally between multiple independent modes can easily be visualized from the single channel curve represented in Fig. 6.

B. Advanced Fibers for Spatial Multiplexing

Spatial multiplexing in fibers requires fibers that guide more than one spatial mode. Fig. 20 shows examples of fibers guiding multiple spatial modes (fibers 2 to 7) along with a single-mode fiber (fiber 1). Fibers 2–4 are multicore fibers (MCFs) with a varying number of cores but following an hexagonal grid [128]–[133]. The hexagonal pattern of cores allows for the most compact placement of the cores for 7 and 19 cores, where all nearest-neighbor cores are separated by the same distance (see the problem of sphere packing in two dimensions [134]). Fibers that have a single large core that can support a few (∼3 to 10) or many (above ∼10) spatial modes are traditionally called multimode fibers (MMFs) [135]–[138]. They are represented by fibers 5 and 6, respectively. Fiber 7 is an example of a photonic bandgap fiber (PBF), the hollow-core fiber (HCF) mentioned in Section IV-E. We discuss these fibers below.

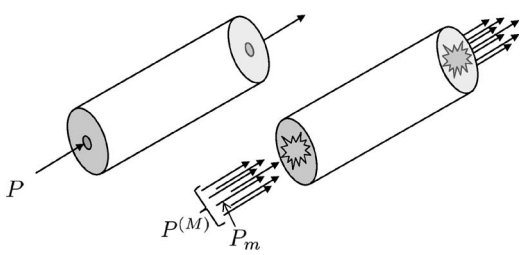

Fig. 19. ***Schematic of a single-mode fiber and of spatial multiplexing in fibers.***

A MCF can be designed in essentially two ways. The first is to try to isolate the cores as much as possible from each other to create uncoupled parallel channels [130], [131], [139], [140]. Each core is considered as an independent channel over which independent data are sent. We refer to such a fiber as low-coupling MCF (LMCF). To achieve this goal, a LMCF is designed to minimize energy transfer between cores from linear coupling. Linear coupling between cores occurs as a consequence of the overlap of individual core modes (considered in isolation) with the index profile of neighboring cores of a MCF. Linear coupling can be suppressed by ensuring the extent of the isolated-core mode to be well within the distance between cores. The overlap of the field associated to one core near the location of a different core can be reduced by reshaping the mode field using specially designed refractive index profiles [131]–[133], [140], [141]. One can also simply reduce the mode field diameter of each of the isolated-core modes without reshaping the mode itself, but this approach has the drawback of decreasing the effective area of each mode and increasing the nonlinear coefficient γ [see definition of γ below (17)]. Smaller mode field diameters can also require more precision in the fabrication of MCFs, such as more precision on the location of each core inside the fiber. These fiber design trade-offs generally lead to the presence of residual crosstalk between cores. Other sources of crosstalk between cores are also present in systems based on MCFs, including crosstalk induced by fiber macrobending [140], [142], spatial multiplexing and demultiplexing, and splicing. Since the cores in a LMCF

are considered independent channels and are processed separately, any source of crosstalk between cores creates an irreversible degradation in performance.

A second design of MCF does not impose any restrictions on the linear coupling between cores, allowing large coupling to occur. We refer to such a fiber as a high-coupling MCF (HMCF). The impact of the high level of crosstalk induced by coupling in HMCF can be largely removed by first performing coherent detection at the output of each core followed by joint digital signal processing of all the fields received using MIMO techniques [26]. This MIMO processing enables recovery of the data with minimum penalty. An experimental demonstration using MIMO processing to transmit nearly penalty-free over 24 km of a three-core HMCF with 4-dB total crosstalk between cores is reported in [143].

Multimode fibers are made from a single core of sufficiently large diameter to support more than one spatial mode. The number of spatial modes guided in a MMF grows rapidly with the core diameter and can number in the hundreds. For an *ideal* MMF, the spatial modes spatially overlap but do not couple and transmission can be performed by using spatial multiplexing and demultiplexing of each individual mode using spatial filters [112]. In practice, coupling between modes occurs due to both macro- [136], [144], [145] and micro-bending [136], [144], [146]–[149]. In a similar manner to the MCFs, MIMO techniques can be applied in combination with coherent detection in MMFs to recover the data even in the presence of large coupling between modes. Experimental realizations of MIMO processing that successfully reduced the impact of coupling between modes in MMF transmission are reported in [150], [151].

It is interesting to consider advanced fibers such as microstructured fibers, or photonics crystal fibers (PCFs), and how they can impact transmission if they mature to become manufacturable in long lengths and at low cost. An example of PCF of interest is the HCF shown in Fig. 20 that can be designed to support a single or multiple spatial modes [152], [153]. Because the core, where most of the spatial mode is confined, is composed of air, HCFs can have an ultra-low nonlinear coefficient [152]. It has been conjectured that HCFs may be able to achieve ultra-low loss, possibly as low as $\sim$0.05 dB/km at a wavelength of 2 μm [104], even though the lowest loss coefficient achieved to date is 0.48 dB/km [153]. The impact of reduced loss and reduced nonlinearity on capacity for single-mode operation has been discussed in Section IV-E. The technique to multiplex and demultiplex spatial modes in and out of a HCF supporting many spatial modes is expected to be similar to other fibers supporting multiple spatial modes.

Finally, one should note that a HMCF can be considered as supporting "supermodes" [154]. These supermodes are the spatial modes calculated taking into account the entire HMCF structure [155], [156] as opposed to considering the HMCF modes as a combination of isolated-core modes. These supermodes are in fact the true modes of the HMCF. Nevertheless, approximations of supermodes using isolated-core modes can be accurate and useful [157]–[161]. Therefore, HMCF, MMF and multimode PBF can be seen as different fiber technologies and designs that can support multiple spatial modes. HMCF and MMF with a large number of modes and low loss ($\sim$0.2 dB/km) have been routinely fabricated while PBFs for long distance transmission have yet to be demonstrated.

C. Capacity of Spatial Multiplexing in Fibers

As mentioned in previous sections, the spatial modes of an *ideal* fiber do not couple to each other during propagation. For such an ideal fiber, each spatial mode can be identified as a channel in the sense of Shannon. However, for practical fibers, linear coupling between modes almost invariably occurs due to imperfections in waveguide, material or due to fiber bending [162]. Such linear mode coupling can occur at various locations along the fiber and with various coupling strengths. Despite this unpredictability in the coupling of individual modes, the overall effect of mode coupling on all modes is not arbitrary and obeys the *coupled-mode theory* (CMT) [138], [163]–[176]. Coupled-mode theory can be applied for instance to the field evolution in each core of a HMCF and to spatial modes in MMF experiencing linear coupling. It has been shown that the matrix of coupling coefficients between modes is Hermitian [175], which makes the corresponding channel transfer matrix unitary. It is well known in information theory that a unitary transformation does not impact channel capacity [27], [30]–[32]. Therefore, the coupling between modes in fibers does not impact capacity and one can use the capacity comparison between a single and M independent AWGN channels developed in Sections V-A and V to assess the potential of spatial multiplexing in fibers.

A variety of phenomena can occur during propagation over fibers that can make capacity differ from the case of independent AWGN channels. The first category involves mode-dependent loss (MDL), and it includes polarization-dependent loss (PDL) [177]–[182] and spatial MDL [183]–[186]. A similar impact on capacity is expected from mode-dependent gain (MDG) such as polarization-dependent gain (PDG) or spatial MDG. Spatial MDL can originate from various sources, including a difference in fiber loss coefficients between spatial modes, a differential in transmission between spatial modes in discrete network elements, such as at the transmitter or receiver, at couplers, at mode multiplexers and demultiplexers, at reconfigurable optical add-drop multiplexers (ROADMs), or at the location of fiber splices. The phenomena of PDG and spatial MDG can only occur at the location of optical amplifiers. Note that the MDLs and MDGs mentioned above can be reduced by advanced fiber and device fabrication techniques.

A second category of phenomena that can affect capacity originates from the Kerr nonlinear effects discussed in Section IV for SMFs. The equations that describe nonlinear propagation need to be generalized to include all possible nonlinear interactions between all modes present [187]–[192]. It is well known that nonlinear interactions between copropagating fields depends mainly on two parameters, the nonlinear overlap between modes [189], [190] and the difference in the modal propagation constants. The nonlinear field overlap terms are proportional to the integral [189] $\iint dx\,dy(\mathbf{F}_p^* \cdot \mathbf{F}_l)(\mathbf{F}_m \cdot \mathbf{F}_n^*)$ or $\iint dx\,dy(\mathbf{F}_p^* \cdot \mathbf{F}_l^*)(\mathbf{F}_m \cdot \mathbf{F}_n)$ where $\mathbf{F}_m(x,y)$ is the transverse field representing the mode labeled m and $\mathbf{F}_m^*$ its complex conjugate. The larger these overlap integrals are, the larger the nonlinear coefficients associated with nonlinear modes interactions. When two fields have similar constants of propagation β, nonlinear interactions between these fields can increase dramatically due to the onset of phase matching conditions that leads to four-wave mixing (FWM) [193], [194] or due to group-velocity matching that lead to a cross-phase modulation (XPM) type process [195], [196]. The difference in constants of propagation between spatial modes is determined mainly by the fiber design and to a lesser extent by fabrication tolerances.

Three scenarios emerge to describe the nonlinear interactions between spatial modes. A first scenario is when the overlap between spatial modes is kept small so as to minimize the nonlinear field overlap terms mentioned above. A second scenario is to allow large overlap between spatial modes, but design a fiber to have a sufficient difference between the constants of propagation so as to minimize nonlinear distortions between modes. The third scenario is to allow spatial modes to overlap and have similar constants of propagation, in which cases nonlinear interactions between modes are expected to be the strongest. It is interesting to note that one can cancel the effects of crosstalk between modes only if the time delay between all the modes allows a realizable implementation of MIMO processing at the receiver. There is therefore a maximum difference of group velocity between modes above which MIMO processing cannot be performed and for which crosstalk cannot be suppressed. There is therefore a trade-off between crosstalk and nonlinearity suppression for spatial multiplexing in fibers. From a fundamental perspective, it is unclear which fiber design that supports multiple spatial modes has maximum capacity.

Increasing the capacity of optical fibers through spatial multiplexing will only have a large impact on system cost if it is possible to similarly increase the capacity of the subsystems attached to the fiber. The development of spatial multiplexing in fibers will require dramatic progress in a broad area of integrated technologies including transceivers, optical amplifiers, wavelength multiplexers and demultiplexers and a variety of other components. A first example of this integration is monolithic receivers designed to simultaneously detect the signals from 7 cores of a MCF [197]. This device received signals on two wavelengths from each core and provided polarization diversity.

VI. NETWORK IMPLICATIONS

The scaling of network traffic and capacity discussed above does not imply that the network itself is scaled; as traffic increases there is not a concomitant increase in the number of nodes or the number of users. This has some implications for the use of optical networking technologies. If fiber capacity were to be limited to that supportable in a single mode, then demands between nodes would need to be served by an increasing number of fibers and the capacity of a fiber would become a smaller and smaller unit as time goes by. This would in turn suggest a diminishing value for optical add/drop technologies since there would eventually be little reason to terminate less than a complete fiber's worth of traffic. If alternatively spatial multiplexing technology enables the scaling of fiber capacity with traffic, new optical add/drop technologies will need to be developed. If fibers with strongly coupled modes or cores are used, then the need for MIMO processing to mitigate against the adding or dropping of individual modes or cores and wavelength-based add/drops of MMF or MCF signals will be needed. In this way the MMF or MCF signal will become a new optical channel and will also allow scaling of the channel rate to speeds beyond 1 Tb/s.

VII. CONCLUSION

In this paper, we presented historical data on fiber capacity and network traffic growths and pointed out that, at the rate of growth of the last decade, network traffic demand is now exceeding the capacity of individual fiber communication systems, reversing the situation that has existed since the beginning of the WDM era. We presented capacity limit estimates of advanced single-mode fibers and showed that even a large reduction in fiber loss or nonlinear coefficients would not be sufficient to double the capacity of standard single-mode fibers. We presented the potential of using spatial multiplexing in fibers supporting multiple spatial modes in combination with multiple-input multiple-output digital signal processing to provide dramatic increase in capacity or reducing the energy of transmission by one to two orders of magnitude. Spatial multiplexing in fibers is the only new fiber technology that can provide the capacity scaling compatible with traffic demands in the next few decades. ■

Acknowledgment

The authors would like to thank J. Foschini, A. Tulino, G. Kramer, R. Ryf, B. Basch, A. Chraplyvy, P. Winzer, C. Xie, X. Liu, H. Kogelnik, and many other Researchers from Bell Laboratories.

REFERENCES

[1] E. B. Basch, *Optical-Fiber Transmission*. Sams Technical Publishing, 1986.

[2] H. Kogelnik, "High-capacity optical communications: Personal recollections," *IEEE J. Sel. Topics Quantum Electron.*, vol. 6, no. 6, pp. 1279–1286, Nov./Dec. 2000.

[3] G. P. Agrawal, *Fiber-Optic Communication Systems*, 3rd ed. Hoboken, NJ: Wiley-Interscience, 2010.

[4] A. H. Gnauck, R. W. Tkach, A. R. Chraplyvy, and T. Li, "High-capacity optical transmission systems," *J. Lightw. Technol.*, vol. 26, no. 9, pp. 1032–1045, May 1, 2008.

[5] R. Tkach, "Scaling optical communications for the next decade and beyond," *Bell Labs Techn. J.*, vol. 14, no. 4, pp. 3–9, 2010.

[6] University of Minnesota, *Minnesota Internet Traffic Studies (MINTS)*. [Online]. Available: http://www.dtc.umn.edu/mints/home.php

[7] B. Swanson and G. Gilder, "Estimating the Exaflood—The impact of video and rich media on the internet—A zettabyte by 2015?" Discovery Institute, Jan. 29, 2008.

[8] C. V. N. Index, "Forecast and Methodology, 2007–2012," White Paper, Cisco Systems, San Jose, CA, Jun. 16, 2008.

[9] C. V. N. Index, "Forecast and Methodology, 2010–2015," White Paper, Cisco Systems, San Jose, CA, Jun. 1, 2011. [Online]. Available: http://www.cisco.com/en/US/solutions/collateral/ns341/ns525/ns537/ns705/ns827/white_paper_c11-481360_ns827_Networking_Solutions_White_Paper.html

[10] A. M. Odlyzko. (2010). Bubbles, gullibility, and other challenges for economics, psychology, sociology, and information sciences. *First Monday*. [Online]. *15(9-6)*. Available: http://ssrn.com/abstract=1668130

[11] [Online]. The list of the Top 500 computers can be found at http://www.Top500.org

[12] J. Gantz and D. Reinsel, "The Digital Universe Decade—Are You Ready?" IDC White Paper, May 2010. [Online]. Available: http://www.emc.com/collateral/analyst-reports/idc-digital-universe-are-you-ready.pdf

[13] H. Onaka, H. Miyata, G. Ishikawa, K. Otsuka, H. Ooi, Y. Kai, S. Kinoshita, M. Seino, H. Nishimoto, and T. Chikama, "1.1 Tb/s WDM transmission over a 150 km, 1.3 μ/m zero-dispersion single-mode fiber," in *Proc. Opt. Fiber Commun. Conf. (OFC)*, PD19, 1996.

[14] A. H. Gnauck, A. R. Chraplyvy, R. W. Tkach, J. L. Zyskind, J. W. Sulhoff, A. J. Lucero, Y. Sun, R. M. Jopson, F. Forghieri, R. M. Derosier, C. Wolf, and A. R. McCormick, "One terabit/s transmission experiment," in *Proc. Opt. Fiber Commun. Conf. (OFC)*, PD20, 1996.

[15] T. Morioka, H. Takara, S. Kawanshi, O. Kamatani, K. Takiguchi, K. Uchiyama, M. Saruwatari, H. Takahashi, M. Yamada, T. Kanamori, and H. Ono, "100 Gbit/s × 10 channel OTDM/WDM transmission using a single supercontinuum WDM source," in *Proc. Opt. Fiber Commun. Conf. (OFC)*, PD21, 1996.

[16] D. Qian, M. Huang, E. Ip, Y. Huang, Y. Shao, J. Hu, and T. Wang, "101.7-Tb/s (370 × 294-Gb/s) PDM-128QAM-OFDM transmission over 3 × 55-km SSMF using pilot-based phase noise mitigation," presented at the Opt. Fiber Commun. Conf. (OFC), 2011, Paper PDPB5.

[17] R.-J. Essiambre, G. Kramer, P. J. Winzer, G. J. Foschini, and B. Goebel, "Capacity limits of optical fiber networks," *J. Lightw. Technol.*, vol. 28, pp. 662–701, 2010.

[18] M. Roughan, A. Greenberg, C. Kalmanek, M. Rumsewicz, J. Yates, and Y. Zhang, "Experience in measuring backbone traffic variability: Models, metrics, measurements and meaning," in *Proc. 2nd ACM SIGCOMM Workshop Internet Measure. (IMW '02)*. ACM, 2002, pp. 91–92.

[19] E. B. Basch, R. A. Beaudette, and H. A. Carnes, "The GTE optical system field trial in Belgium," *Proc. NTC*, pp. 5.3.1–5.3.5, 1978.

[20] E. B. Basch, R. A. Beaudette, H. A. Carnes, and R. F. Kearns, "Aspects of operational fiber optic systems," in *Proc. IEEE Int. Conf. Commun.*, no. 8, pp. 19.6.1–19.6.7, 1979.

[21] E. B. Basch, R. A. Beaudette, H. A. Carnes, and R. F. Kearns, "Aspects of fiber optic interoffice trunks," in *Proc. IEEE Commun. Syst. Seminar*, no. 8, pp. 20–25, 1979.

[22] C. E. Shannon, "A mathematical theory of communication," *The Bell Syst. Technol. J.*, vol. 27, pp. 379–423, 623–656, 1948.

[23] R. G. Gallager, *Information Theory and Reliable Communication*. Hoboken, NJ: Wiley, 1968.

[24] D. J. C. MacKay, *Information Theory, Inference and Learning Algorithms*. Cambridge, U.K.: Cambridge Univ. Press, 2003.

[25] T. M. Cover and J. A. Thomas, *Elements of Information Theory*, 2nd ed. Hoboken, NJ: Wiley, 2006.

[26] G. J. Foschini, "Layered space-time architecture for wireless communication in a fading environment when using multi-element antennas," *Bell Labs Technol. J.*, vol. 1, pp. 41–59, 1996.

[27] I. E. Telatar, "Capacity of multiantenna Gaussian channels," *Eur. Trans. Telecommun.*, vol. 10, no. 6, pp. 585–595, 1999.

[28] S. Benedetto and E. Biglieri, *Principles of Digital Transmission With Wireless Applications*. New York: Kluwer Academic/Plenum Publishers, 1999.

[29] T. S. Rappaport, *Wireless Communications: Principles and Practice*. Englewood Cliffs, NJ: Prentice Hall, 2002.

[30] D. Tse and P. Viswanath, *Fundamentals of Wireless Communication*. Cambridge, U.K.: Cambridge Univ. Press, 2005.

[31] A. Goldsmith, *Wireless Communications*. Cambridge, U.K.: Cambridge Univ. Press, 2005.

[32] A. F. Molisch, *Wireless Communications*. Hoboken, NJ: Wiley, 2005.

[33] S. Hranilovič, *Wireless Optical Communication Systems*. Berlin, Germany: Springer-Verlag, 2005.

[34] I. Kalet and S. Shamai, "On the capacity of a twisted-wire pair: Gaussian model," *IEEE Trans. Commun.*, vol. 38, no. 3, pp. 379–383, Mar. 1990.

[35] J. J. Werner, "The HDSL environment," *IEEE J. Sel. Areas Commun.*, vol. 9, no. 6, pp. 785–800, Nov./Dec. 1991.

[36] M. Gagnaire, "An overview of broad-band access technologies," *Proc. IEEE*, vol. 85, no. 12, pp. 1958–1972, Dec. 1997.

[37] A. Sendonaris, V. V. Veeravalli, and B. Aazhang, "Joint signaling strategies for approaching the capacity of twisted-pair channels," *IEEE Trans. Commun.*, vol. 46, no. 5, pp. 673–685, May 1998.

[38] W. Rhee and J. M. Cioffi, "Increase in capacity of multiuser OFDM system using dynamic subchannel allocation," in *Veh. Technol. Conf. Proc.*, 2000, vol. 2, pp. 1085–1089.

[39] J. D. Gibson, Ed., *The Communications Handbook*. Boca Raton, FL: CRC Press, 1997.

[40] J. P. Gordon, "Quantum effects in communications systems," *Proc. IRE*, vol. 50, pp. 1898–1908, 1962.

[41] J. Pierce, "Optical channels: Practical limits with photon counting," *IEEE Trans. Commun.*, vol. 26, no. 12, pp. 1819–1821, Dec. 1978.

[42] J. Massey, "Capacity, cutoff rate, and coding for a direct-detection optical channel," *IEEE Trans. Commun.*, vol. 29, no. 11, pp. 1615–1621, Nov. 1981.

[43] A. D. Wyner, "Capacity and error exponent for the direct detection photon channel—Part I," *IEEE Trans. Inf. Theory*, vol. 34, no. 6, pp. 1449–1461, Jun. 1988.

[44] A. D. Wyner, "Capacity and error exponent for the direct detection photon channel—Part II," *IEEE Trans. Inf. Theory*, vol. 34, no. 6, pp. 1462–1471, Jun. 1988.

[45] S. Shamai, "Capacity of a pulse amplitude modulated direct detection photon channel," *IEE Proc. Part I: Commun., Speech, Vis.*, vol. 137, no. 6, pp. 424–430, 1990.

[46] H. Hemmati, Ed., *Deep Space Optical Communications*. Hoboken, NJ: Wiley, 2006.

[47] D. O. Caplan, "Laser communication transmitter and receiver design," *J. Opt. Fiber Commun. Res.*, vol. 4, no. 4, pp. 225–362, 2007.

[48] J. G. Proakis and M. Salehi, *Digital Communications*, 5th ed. New York: McGraw Hill, 2007.

[49] S. Haykin, *Communication Systems*, 5th ed. Hoboken, NJ: Wiley, 2009.

[50] H. Nyquist, "Certain factors affecting telegraph speed," *Bell Syst. Techn. J.*, vol. 3, pp. 324–346, 1924.

[51] H. Nyquist, "Certain topics of telegraph transmission theory," *Trans. Amer. Inst. Electr. Eng.*, vol. 47, pp. 617–644, 1928.

[52] R. V. L. Hartley, "Certain factors affecting telegraph speed," *Bell Syst. Tech. J.*, vol. 7, pp. 535–563, 1928.

[53] R.-J. Essiambre, G. J. Foschini, G. Kramer, and P. J. Winzer, "Capacity limits of information transmission in optically-routed fiber networks," *Bell Labs Tech. J.*, vol. 14, no. 4, pp. 149–162, 2010.

[54] J. B. Stark, "Fundamental limits of information capacity for optical communications channels," in *Proc. Eur. Conf. Opt. Commun. (ECOC)*, 1999, no. 4, p. I-28.

[55] F. T. S. Yu, *Entropy and Information Optics*. New York: Marcel Dekker, 2000.

[56] J. Tang, "The Shannon channel capacity of dispersion-free nonlinear optical fiber transmission," *J. Lightw. Technol.*, vol. 19, pp. 1104–1109, Aug. 2001.

[57] P. P. Mitra and J. B. Stark, "Nonlinear limits to the information capacity of optical fibre communications," *Nature*, vol. 411, pp. 1027–1030, 2001.

[58] E. Desurvire, "A quantum model for optically amplified nonlinear transmission systems," *Opt. Fiber Technol.*, pp. 210–230, 2002.

[59] E. Desurvire, "A common quantum noise model for optical amplification and nonlinearity in WDM transmission,"

presented at the Eur. Conf. on Opt. Commun. (ECOC), 2002, Paper Tu3.1.1.

[60] J. Tang, "The channel capacity of a multispan DWDM system employing dispersive nonlinear optical fibers and an ideal coherent optical receiver," *J. Lightw. Technol.*, vol. 20, pp. 1095–1101, Jul. 2002.

[61] K.-P. Ho, "Channel capacity of WDM systems using constant-intensity modulation formats," presented at the Opt. Fiber Commun. Conf. (OFC), 2002, Paper ThGG85.

[62] E. Narimanov and P. P. Mitra, "The channel capacity of a fiber optics communication system: Perturbation theory," *J. Lightw. Technol.*, vol. 20, pp. 530–537, Mar. 2002.

[63] K. S. Turitsyn, S. A. Derevyanko, I. V. Yurkevich, and S. K. Turitsyn, "Information capacity of optical fiber channels with zero average dispersion," *Phys. Rev. Lett.*, vol. 91, 2003, Paper 203901.

[64] J. M. Kahn and K.-P. Ho, "Spectral efficiency limits and modulation/detection techniques for DWDM systems," *IEEE J. Sel. Topics Quantum Electron.*, vol. 10, pp. 259–272, Oct. 2004.

[65] L. G. L. Wegener, M. L. Povinelli, A. G. Green, P. P. Mitra, J. B. Stark, and P. B. Littlewood, "The effect of propagation nonlinearities on the information capacity of WDM optical fiber systems: Cross-phase modulation and four-wave mixing," *Physica D*, vol. 189, pp. 81–99, 2004.

[66] I. Djordjevica, B. Vasic, M. Ivkovic, and I. Gabitov, "Achievable information rates for high-speed long-haul optical transmission," *J. Lightw. Technol.*, vol. 23, pp. 3755–3763, Nov. 2005.

[67] M. H. Taghavi, G. C. Papen, and P. H. Siegel, "On the multiuser capacity of WDM in a nonlinear optical fiber: Coherent communication," *IEEE Trans. Inf. Theory*, vol. 52, no. 11, pp. 5008–5022, Nov. 2006.

[68] M. Ivkovic, I. Djordjevic, and B. Vasic, "Calculation of achievable information rates of long-haul optical transmission systems using instanton approach," *J. Lightw. Technol.*, vol. 25, no. 5, pp. 1163–1168, May 2007.

[69] R.-J. Essiambre, G. J. Foschini, P. J. Winzer, G. Kramer, and E. C. Burrows, "The capacity of fiber-optic communication systems," presented at the Opt. Fiber Commun. Conf. (OFC), 2008, Paper OTuE1.

[70] R.-J. Essiambre, G. J. Foschini, G. Kramer, and P. J. Winzer, "Capacity limits of information transport in fiber-optic networks," *Phys. Rev. Lett.*, vol. 101, 2008, Paper 163901.

[71] R.-J. Essiambre, G. J. Foschini, P. J. Winzer, and G. Kramer, "Exploring capacity limits of fibre-optic communication systems," presented at the Eur. Conf. on Opt. Commun. (ECOC), 2008, Paper We1.E.1.

[72] R.-J. Essiambre, G. Kramer, G. J. Foschini, and P. J. Winzer, "High spectral efficiency modulation for high capacity transmission," presented at the IEEE/LEOS Summer Topical Meeting, 2008, Paper TuC2.2, pp. 113–114.

[73] R.-J. Essiambre, G. J. Foschini, P. J. Winzera, and G. Kramer, "Capacity limits of fiber-optic communication systems," presented at the Opt. Fiber Commun. Conf. (OFC), 2009, p. OThL1.

[74] I. Djordjevic, L. Xu, and T. Wang, "On the channel capacity of multilevel modulation schemes with coherent detection," presented at the Asia Commun. Photon. Conf. Exhibition, 2009, Paper ThC4.

[75] E. Desurvire, *Classical and Quantum Information Theory*. Cambridge, U.K.: Cambridge Univ. Press, 2009.

[76] H. Haunstein and M. Mayrock, "OFDM spectral efficiency limits from fiber and system non-linearities," presented at the Opt. Fiber Commun. Conf. (OFC), 2010, Paper OThM7.

[77] I. Djordjevic, "Ultimate information capacity of fiber optic networks," in *SPIE Photon. West*, 2010, no. 4, p. 7621-19.

[78] A. Ellis, J. Zhao, and D. Cotter, "Approaching the non-linear Shannon limit," *J. Lightw. Technol.*, vol. 28, no. 4, pp. 423–433, Feb. 15, 2010.

[79] I. Djordjevic, W. Ryan, and B. Vasic, "Optical channel capacity," in *Coding for Optical Channels*. Berlin, Germany: Springer-Verlag, 2010, pp. 353–398.

[80] R. Stolen, "Nonlinearity in fiber transmission," *Proc. IEEE*, vol. 68, no. 10, pp. 1232–1236, Oct. 1980.

[81] A. R. Chraplyvy, "Limitations on lightwave communications imposed by optical-fiber nonlinearities," *J. Lightw. Technol.*, vol. 8, pp. 1548–1557, Oct. 1990.

[82] R.-J. Essiambre, G. Raybon, and B. Mikkelsen, "Pseudo-linear transmission of high-speed TDM signals: 40 and 160 Gb/s," in *Opt. Fiber Telecommun. IV*, I. Kaminow and T. Li, Eds. New York: Academic Press, 2002, pp. 232–304.

[83] G. P. Agrawal, *Nonlinear Fiber Optics*, 4th ed. San Diego: Elsevier Science & Technology, 2006.

[84] G. J. Foschini and M. J. Gans, "On limits of wireless communications in a fading environment when using multiple antennas," *Wireless Personal Commun.*, vol. 6, no. 3, pp. 311–335, 1998.

[85] J. Kerr, "On rotation of the plane of polarization by reflection from the pole of a magnet," *Phil. Mag.*, vol. 3, no. 19, pp. 321–343, 1877.

[86] R.-J. Essiambre and P. J. Winzer, "Fibre nonlinearities in electronicaly pre-distorted transmission," presented at the Eur. Conf. Opt. Commun. (ECOC), 2005, Paper Tu3.2.2.

[87] R. Essiambre and P. Winzer, "Impact of fiber nonlinearities on advanced modulation formats using electronic pre-distortion," presented at the Opt. Fiber Commun. Conf. (OFC), 2006, Paper OWB1.

[88] R.-J. Essiambre, P. J. Winzer, X. Q. Wang, W. Lee, C. A. White, and E. C. Burrows, "Electronic predistortion and fiber nonlinearity," *Photon. Technol. Lett.*, vol. 18, no. 17, pp. 1804–1806, Sep. 2006.

[89] L. F. Mollenauer and J. P. Gordon, *Solitons in Optical Fibers: Fundamentals and Applications*. New York: Academic Press, 2006.

[90] J. P. Gordon, W. H. Louisell, and L. R. Walker, "Quantum fluctuations and noise in parametric processes II," *Phys. Rev.*, vol. 129, pp. 481–485, 1963.

[91] J. P. Gordon, L. R. Walker, and W. H. Louisell, "Quantum statistics of masers and attenuators," *Phys. Rev.*, vol. 130, pp. 806–812, 1963.

[92] J. R. Barry, D. G. Messerschmitt, and E. A. Lee, *Digital Commun.*, 5th ed. Berlin, Germany: Springer, 2003.

[93] A. Mecozzi, "Limits to long-haul coherent transmission set by the Kerr nonlinearity and noise of the in-line amplifiers," *J. Lightw. Technol.*, vol. 12, pp. 1993–2000, Nov. 1994.

[94] C. W. Gardiner, *Handbook of Stochastic Methods: For Physics, Chemistry and the Natural Science*, 3rd ed. Berlin, Germany: Springer-Verlag, 2004.

[95] C. W. Gardiner and P. Zoller, *Quantum Noise: A Handbook of Markovian and Non-Markovian Quantum Stochastic Methods With Applications to Quantum Optics*, 3rd ed. Berlin, Germany: Springer-Verlag, 2004.

[96] N. W. Ashcroft and N. D. Mermin, *Solid State Physics*, vol. 826. Pacific Grove, CA: Brooks Cole, 1976.

[97] J. Bromage, "Raman amplification for fiber communications systems," *J. Lightw. Technol.*, vol. 22, pp. 79–93, Jan. 2004.

[98] H. Takahashi, A. A. Amin, S. L. Jansen, I. Morita, and H. Tanaka, "DWDM transmission with 7.0 bit/s/Hz spectral efficiency using 8 × 65.1 Gbit/s coherent PDM OFDM signals," presented at the Opt. Fiber Commun. Conf. (OFC), 2009, Paper PDPB7.

[99] A. H. Gnauck, P. J. Winzer, C. R. Doerr, and L. L. Buhl, "10 × 112-Gb/s PDM 16-QAM transmission over 630 km of fiber with 6.2-b/s/Hz spectral efficiency," presented at the Opt. Fiber Commun. Conf. (OFC), 2009, Paper PDPB8.

[100] A. Sano, H. Masuda, T. Kobayashi, M. Fujiwara, K. Horikoshi, E. Yoshida, Y. Miyamoto, M. Matsui, M. Mizoguchi, H. Yamazaki, Y. Sakamaki, and H. Ishii, "69.1-Tb/s (432 × 171-Gb/s) C- and extended L-band transmission over 240 km using PDM-16-QAM modulation and digital coherent detection," presented at the Opt. Fiber Commun. Conf. (OFC), 2010, Paper PDPB7.

[101] X. Zhou, J. Yu., M.-F. Huang, Y. Shao, T. Wang, L. Nelson, P. Magill, M. Birk, P. I. Borel, D. W. Peckham, and R. Lingle, Jr., "64-Tb/s (640 × 107-Gb/s) C- PDM-36 QAM transmission over 320 km using both pre- and post-transmission digital equalization," presented at the Opt. Fiber Commun. Conf. (OFC), 2010, Paper PDPB9.

[102] A. Sano, T. Kobayashi, A. Matsuura, S. Yamamoto, S. Yamanaka, E. Yoshida, Y. Miyamoto, M. Matsui, M. Mizoguchi, and T. Mizuno, "100 × 120-Gb/s PDM 64-QAM transmission over 160 km using linewidth-tolerant pilotless digital coherent detection," presented at the Eur. Conf. Opt. Commun. (ECOC), 2010, Paper PD2.4.

[103] K. Nagayamaa, M. Kakui, M. Matsui, I. Saitoh, and Y. Chigusa, "Ultra-low-loss (0.1484 dB/km) pure silica core fibre and extension of transmission distance," *IEE Electron. Lett.*, vol. 38, no. 20, pp. 1168–1169, 2002.

[104] P. J. Roberts, F. Couny, H. Sabert, B. J. Mangan, D. P. Williams, L. Farr, M. W. Mason, A. Tomlinson, T. A. Birks, J. C. Knight, and P. S. J. Russell, "Ultimate low loss of hollow-core photonic crystal fibres," *Opt. Exp.*, vol. 13, no. 1, pp. 236–244, 2005.

[105] P. C. Becker, N. A. Olsson, and J. R. Simpson, *Erbium-Doped Fiber Amplifiers, Fundamentals and Technology*. New York: Academic Press, 1999.

[106] E. Desurvire, D. Bayart, B. Desthieux, and S. Bigo, *Erbium-Doped Fiber Amplifiers and Device and System Developments*. Hoboken, NJ: Wiley, 2002.

[107] D. G. Ouzounov, F. R. Ahmad, D. Müller, N. Venkataraman, M. T. Gallagher, M. G. Thomas, J. Silcox, K. W. Koch, and A. L. Gaeta, "Generation of megawatt optical solitons in hollow-core photonic band-gap fibers," *Science*, vol. 301, no. 5640, p. 1702, 2003.

[108] A. R. Bhagwat and A. L. Gaeta, "Nonlinear optics in hollow-core photonic bandgap fibers," *Opt. Exp.*, vol. 16, no. 7, pp. 5035–5047, 2008.

[109] K. Thyagarajan and A. Ghatak, *Fiber Optic Essentials*. Hoboken, NJ: Wiley-Interscience, 2007.

[110] B. E. A. Saleh and M. C. Teich, *Fundamentals of Photonics*, 2nd ed. Hoboken, NJ: Wiley-Interscience, 2007.

[111] G. Keiser, *Optical Fiber Communications*, 3rd ed. New York: McGraw Hill, 2000.

[112] R. Ryf, "Optical coupling components for spatial multiplexing in multi-mode fibers," presented at the Eur. Conf. Opt. Commun. (ECOC), Th.12.B.1, 2011.

[113] J. Wang, S. Zhua, and L. Wang, "On the channel capacity of MIMO-OFDM systems," in *IEEE Int. Symp. Commun. Inf. Technol.*, 2005, vol. 2, pp. 1372–1375.

[114] E. Biglieri, R. Calderbank, and A. Constantinides, *MIMO Wireless Communications*. Cambridge, U.K.: Cambridge Univ. Press, 2007.

[115] C. Oestges and B. Clerckx, *MIMO Wireless Communications: From Real-World Propagation to Space-Time Code Design*. New York: Academic Press, 2007.

[116] H. R. Stuart, "Dispersive multiplexing in multimode optical fiber," *Science*, vol. 289, no. 5477, pp. 281–283, 2000.

[117] H. Bölcskei, D. Gesbert, and A. J. Paulraj, "On the capacity of OFDM-based spatial multiplexing systems," *IEEE Trans. Commun.*, vol. 50, no. 2, pp. 225–234, Feb. 2002.

[118] S. Verdú, "Spectral efficiency in the wideband regime," *IEEE Trans. Inf. Theory*, vol. 48, no. 6, pp. 1319–1343, Jun. 2002.

[119] R. C. J. Hsu, A. Tarighat, A. Shah, A. H. Sayed, and B. Jalali, "Capacity enhancement in coherent optical MIMO (COMIMO) multimode fiber links," *IEEE Commun. Lett.*, vol. 10, no. 3, pp. 195–197, Mar. 2006.

[120] A. Tarighat, R. Hsu, A. Shah, A. Sayed, and B. Jalali, "Fundamentals and challenges of optical multiple-input multiple-output multimode fiber links," *IEEE Commun. Mag.*, vol. 45, no. 5, pp. 57–63, May 2007.

[121] I. B. Djordjevic, M. Arabaci, L. Xu, and T. Wang, "Spatial-domain-based multidimensional modulation for multi-Tb/s serial optical transmission," *Opt. Exp.*, vol. 19, no. 7, pp. 6845–6857, 2011.

[122] A. Lozano, A. M. Tulino, and S. Verdú, "Multiple-antenna capacity in the low-power regime," *IEEE Trans. Inf. Theory*, vol. 49, no. 10, pp. 2527–2544, Oct. 2003.

[123] S. K. Jayaweera, "An energy-efficient virtual MIMO architecture based on V-BLAST processing for distributed wireless sensor networks," in *Proc. IEEE Sensor Ad Hoc Commun. Netw. Conf.*, 2003, pp. 299–308.

[124] S. Cui, A. J. Goldsmith, and A. Bahai, "Energy-efficiency of MIMO and cooperative MIMO techniques in sensor networks," *IEEE J. Sel. Areas Commun.*, vol. 22, no. 6, pp. 1089–1098, Nov./Dec. 2004.

[125] S. Cui, A. J. Goldsmith, and A. Bahai, "Energy-constrained modulation optimization," *IEEE Trans. Wireless Commun.*, vol. 4, no. 5, pp. 2349–2360, May 2005.

[126] P. J. Winzer, "Energy-efficient optical transport capacity scaling through spatial multiplexing," *Photon. Technol. Lett.*, vol. 23, no. 13, pp. 851–853, Jul. 1, 2011.

[127] I. B. Djordjevic, "Energy-efficient spatial-domain-based hybrid multidimensional coded-modulations enabling multi-Tb/s optical transport," *Opt. Exp.*, vol. 19, no. 17, pp. 16 708–16 714, 2011.

[128] S. Inao, T. Sato, S. Sentsui, T. Kuroha, and Y. Nishimura, "Multicore optical fiber," presented at the Opt. Fiber Commun. Conf. (OFC), WB1, 1979.

[129] M. Koshiba, K. Saitoh, and Y. Kokubun, "Heterogeneous multi-core fibers: Proposal and design principle," *IEICE Electron. Exp.*, vol. 6, no. 2, pp. 98–103, 2009.

[130] B. Zhu, T. F. Taunay, M. F. Yan, J. M. Fini, M. Fishteyn, E. M. Monberg, and F. V. Dimarcello, "Seven-core multicore fiber transmissions for passive optical network," *Opt. Exp.*, vol. 18, no. 11, pp. 11 117–11 122, 2010.

[131] J. M. Fini, T. Taunay, B. Zhu, and M. Yan, "Low cross-talk design of multi-core fibers," in *Proc. Conf. Lasers Electro-optics*, 2010.

[132] T. Hayashi, T. Taru, O. Shimakawa, T. Sasaki, and E. Sasaoka, "Low-crosstalk and low-loss multi-core fiber utilizing fiber bend," presented at the Opt. Fiber Commun. Conf. (OFC), OWJ3, 2011.

[133] T. Hayashi, T. Taru, O. Shimakawa, T. Sasaki, and E. Sasaoka, "Ultra-low-crosstalk multi-core fiber feasible to ultra-long-haul transmission," presented at the Opt. Fiber Commun. Conf. (OFC), PDPC2, 2011.

[134] J. H. Conway and N. J. A. Sloane, *Sphere Packings, Lattices, and Groups*, 3rd ed. Berlin, Germany: Springer-Verlag, 2010.

[135] D. Gloge, "Optical power flow in multimode fibers,," *Bell Syst. Tech. J.*, vol. 51, pp. 1767–1783, 1972.

[136] D. Gloge, "Bending loss in multimode fibers with graded and ungraded core index," *Appl. Opt.*, vol. 11, no. 11, pp. 2506–2513, 1972.

[137] D. Gloge and E. A. J. Marcatili, "Multimode theory of graded-core fibers," *Bell Syst. Techn. J.*, vol. 52, pp. 1563–1578, 1973.

[138] D. Marcuse, *Theory of Dielectric Optical Waveguides*, P. F. Liao and P. L. Kelley, Eds. New York: Academic Press, 1991.

[139] Y. Kokubun and M. Koshiba, "Novel multi-core fibers for mode division multiplexing: Proposal and design principle," *IEICE Electron. Exp.*, vol. 6, no. 8, pp. 522–528, 2009.

[140] K. Imamura, K. Mukasa, and T. Yagi, "Investigation on multi-core fibers with large aeff and low micro bending loss," presented at the Opt. Fiber Commun. Conf. (OFC), OWK6, 2010, Paper OThM7.

[141] B. Zhu, T. F. Taunay, M. Fishteyn, X. Liu, S. Chandrasekhar, M. F. Yan, J. M. Fini, E. M. Monberg, and F. V. Dimarcello, "Space-, wavelength-, polarization-division multiplexed transmission of 56 Tb/s over a 76.8 km seven-core fiber," presented at the Opt. Fiber Commun. Conf. (OFC), PDPB7, 2011.

[142] J. M. Fini, B. Zhu, T. F. Taunay, and M. F. Yan, "Statistics of crosstalk in bent multicore fibers," *Opt. Exp.*, vol. 18, no. 14, pp. 15 122–15 129, 2010.

[143] R. Ryf, R.-J. Essiambre, S. Randel, A. H. Gnauck, P. J. Winzer, T. Hayashi, T. Taru, and T. Sasaki, "MIMO-based crosstalk suppression in spatially multiplexed 56-Gb/s PDM-QPSK signals in strongly-coupled 3-core fiber," *Photon. Technol. Lett.*, vol. 23, no. 7, Jul. 2011.

[144] R. Olshansky, "Mode coupling effects in graded-index optical fibers," *Appl. Opt.*, vol. 14, no. 4, pp. 935–945, 1975.

[145] D. Marcuse, "Curvature loss formula for optical fibers," *J. Opt. Soc. Amer.*, vol. 66, no. 3, pp. 216–220, 1976.

[146] D. Marcuse, "Coupled mode theory of round optical fibers," *Bell Syst. Techn. J.*, vol. 52, no. 6, pp. 817–842, 1973.

[147] W. B. Gardner, "Microbending loss in optical fibers," *Bell Syst. Tech. J.*, vol. 54, no. 2, pp. 457–465, 1975.

[148] L. Jeunhomme and J. P. Pocholle, "Mode coupling in a multimode optical fiber with microbends," *Appl. Opt.*, vol. 14, no. 10, pp. 2400–2405, 1975.

[149] L. Su, K. Chiang, and C. Lu, "Microbend-induced mode coupling in a graded-index multimode fiber," *Appl. Opt.*, vol. 44, no. 34, pp. 7394–7402, 2005.

[150] R. Ryf, S. Randel, A. H. Gnauck, C. Bolle, R.-J. Essiambre, P. J. Winzer, D. W. Peckham, A. McCurdy, and R. Lingle, Jr., "Space-division multiplexing over 10 km of three-mode fiber using coherent 6 × 6 MIMO processing," presented at the Opt. Fiber Commun. Conf. (OFC), PDPB10, 2011.

[151] M. Salsi, C. Koebele, D. Sperti, P. Tran, P. Brindel, H. Mardoyan, S. Bigo, A. Boutin, F. Verluise, P. Sillard, M. Bigot-Astruc, L. Provost, F. Cerou, and G. Charlet, "Transmission at 2 × 100 Gb/s, over two modes of 40 km-long prototype few-mode fiber, using LCOS based mode multiplexer and demultiplexer," presented at the Opt. Fiber Commun. Conf. (OFC), PDPB9, 2011.

[152] R. F. Cregan, B. J. Mangan, J. C. Knight, T. A. Birks, P. S. J. Russell, P. J. Roberts, and D. C. Allan, "Single-mode photonic band gap guidance of light in air," *Science*, vol. 285, no. 5433, pp. 1537–1539, 1999.

[153] M. Nielsen, C. Jacobsen, N. Mortensen, J. Folkenberg, and H. Simonsen, "Low-loss photonic crystal fibers for transmission systems and their dispersion properties," *Opt. Exp.*, vol. 12, no. 7, pp. 1372–1376, 2004.

[154] E. Kapon, J. Katz, and A. Yariv, "Supermode analysis of phase-locked arrays of semiconductor lasers," *Opt. Lett.*, vol. 9, no. 4, pp. 125–127, 1984.

[155] Y. Huo, P. K. Cheo, and G. G. King, "Fundamental mode operation of a 19-core phase-locked Yb-doped fiber amplifier," *Opt. Exp.*, vol. 12, no. 25, pp. 6230–6239, 2004.

[156] Y. Huo and P. K. Cheo, "Analysis of transverse mode competition and selection in multicore fiber lasers," *J. Opt. Soc. Amer. B*, vol. 22, no. 11, pp. 2345–2349, 2005.

[157] E. Yamashita, S. Ozeki, and K. Atsuki, "Modal analysis method for optical fibers with symmetrically distributed multiple cores," *J. Lightw. Technol.*, vol. 3, no. 2, pp. 341–346, Apr. 1985.

[158] N. Kishi, E. Yamashita, and K. Atsuki, "Modal and coupling field analysis of optical fibers with circularly distributed multiple cores and a central core," *J. Lightw. Technol.*, vol. 4, no. 8, pp. 991–996, Aug. 1986.

[159] A. J. Stevenson and J. D. Love, "Vector modes of six-port couplers," *IEE Electron. Lett.*, vol. 23, no. 19, pp. 1011–1013, 1987.

[160] N. Kishi and E. Yamashita, "A simple coupled-mode analysis method for multiple-core optical fiber and coupled dielectric waveguide structures," *IEEE Trans. Microw. Theory Technol.*, vol. 36, no. 12, pp. 1861–1868, Dec. 1988.

[161] R. J. Black and L. Gagnon, *Optical Waveguide Modes: Polarization, Coupling and Symmetry*. New York: McGraw-Hill, 2009.

[162] J. A. Buck, *Fundamentals of Optical Fibers*. Hoboken, NJ: Wiley-IEEE, 2004.

[163] S. E. Miller, "Coupled wave theory and waveguide applications," *Bell Syst. Tech. J.*, vol. 33, pp. 661–719, 1954.

[164] J. R. Pierce, "Coupling of modes of propagation," *J. Appl. Phys.*, vol. 25, no. 2, pp. 179–183, 1954.

[165] H. E. Rowe and D. T. Young, "Transmission distortion in multimode random waveguides," *IEEE Trans. Microw. Theory Technol.*, vol. 20, no. 6, pp. 349–365, Jun. 1972.

[166] J. A. Morrison and J. McKenna, "Coupled line equations with random coupling," *Bell Syst. Tech. J.*, vol. 51, no. 1, pp. 209–228, 1972.

[167] D. Marcuse, "Derivation of coupled power equations," *Bell Syst. Tech. J.*, vol. 51, no. 1, pp. 229–237, 1972.

[168] A. W. Snyder, "Coupled-mode theory for optical fibers," *J. Opt. Soc. Amer.*, vol. 62, no. 11, pp. 1267–1277, 1972.

[169] A. Yariv, "Coupled-mode theory for guided-wave optics," *IEEE J. Quantum Electron.*, vol. 9, no. 9, pp. 919–933, Sep. 1973.

[170] A. Hardy and W. Streifer, "Coupled mode solutions of multiwaveguide systems," *IEEE J. Quantum Electron.*, vol. 22, no. 4, pp. 528–534, Apr. 1986.

[171] A. Hardy and W. Streifer, "Coupled modes of multiwaveguide systems and phased arrays," *J. Lightw. Technol.*, vol. 4, no. 1, pp. 90–99, Jan. 1986.

[172] H. Haus, W. Huang, S. Kawakami, and N. Whitaker, "Coupled-mode theory of optical waveguides," *J. Lightw. Technol.*, vol. 5, no. 1, pp. 16–23, Jan. 1987.

[173] H. Kogelnik, "Theory of optical waveguides," in *Guided-Wave Optoelectronics*, 2nd ed. Berlin, Germany: Springer-Verlag, 1988, pp. 7–88.

[174] H. A. Haus and W. Huang, "Coupled-mode theory," *Proc. IEEE*, vol. 79, no. 10, pp. 1505–1518, Oct. 1991.

[175] W. P. Huang and L. Li, "Coupled-mode theory for optical waveguides: An overview," *J. Opt. Soc. Amer. A*, vol. 11, no. 3, pp. 963–983, 1994.

[176] J. N. Kutz, J. A. Cox, and D. Smith, "Mode mixing and power diffusion in multimode optical fibers," *J. Lightw. Technol.*, vol. 16, no. 7, pp. 1195–1202, Jul. 1998.

[177] A. Nafta, E. Meron, and M. Shtaif, "Capacity limitations in fiber-optic communication systems as a result of polarization-dependent loss," *Opt. Lett.*, vol. 34, no. 23, pp. 3613–3615, 2009.

[178] S. Mumtaz, G. Othman, and Y. Jaouën, "Space-time codes for optical fiber communication with polarization multiplexing," in *Proc. IEEE Int. Conf. Commun.*, 2010, pp. 1–5.

[179] E. Meron, A. Andrusier, M. Feder, and M. Shtaif, "Use of space-time coding in coherent polarization-multiplexed systems suffering from polarization-dependent loss," *Opt. Lett.*, vol. 35, no. 21, pp. 3547–3549, 2010.

[180] S. Mumtaz, Y. Rekaya-Ben, G. Othman, and Jaouën, "PDL mitigation in PolMux OFDM systems using golden and silver polarization-time codes," presented at the Opt. Fiber Commun. Conf. (OFC), 2010, Paper JThA7.

[181] E. Matarazzo and M. Mayrock, "Capacity loss due to polarization effects in coherent optical systems," presented at the Eur. Conf. on Opt. Commun. (ECOC), 2010, Paper 4.19.

[182] E. Meron, A. Andrusier, M. Feder, and M. Shtaif, "Increasing the PDL tolerance of systems by use of the golden-code," presented at the Eur. Conf. Opt. Commun. (ECOC), 2010, Paper 4.12.

[183] H. Blow, "Coherent multi channel transmission over multimode-fiber and related signal processing," presented at the Access Netw. In-House Commun., 2010, Paper 4.04.

[184] H. Bülow, H. Al-Hashimi, and B. Schmauss, "Stable coherent mimo transport over few mode fiber enabled by an adiabatic mode splitter," presented at the Eur. Conf. Opt. Commun. (ECOC), 2010, Paper 4.04.

[185] P. J. Winzer and G. J. Foschini, "Outage calculations for spatially multiplexed fiber links," presented at the Opt. Fiber Commun. Conf. (OFC), OThO5, 2011.

[186] P. J. Winzer and G. J. Foschini, "MIMO capacities and outage probabilities in spatially multiplexed optical transport systems," *Opt. Exp.*, vol. 19, no. 17, pp. 16 680–16 696, 2011.

[187] B. Crosignani and P. Di Porto, "Soliton propagation in multimode optical fibers," *Opt. Lett.*, vol. 6, pp. 329–331, 1981.

[188] B. Crosignani, A. Cutolo, and P. Di Porto, "Coupled-mode theory of nonlinear propagation in multimode and single-mode fibers: Envelope solitons and self-confinement," *J. Opt. Soc. Amer.*, vol. 72, no. 9, pp. 1136–1141, 1982.

[189] F. Poletti and P. Horak, "Description of ultrashort pulse propagation in multimode optical fibers," *J. Opt. Soc. Amer. B*, vol. 25, no. 10, pp. 1645–1654, 2008.

[190] F. Poletti and P. Horak, "Dynamics of femtosecond supercontinuum generation in multimode fibers," *Opt. Exp.*, vol. 17, no. 8, pp. 6134–6147, 2009.

[191] C. Koebele, M. Salsi, G. Charlet, and S. Bigo, "Nonlinear effects in long-haul transmission over bimodal optical fibre," presented at the Eur. Conf. Opt. Commun. (ECOC), Mo.2.C.6, 2010.

[192] C. Koebele, M. Salsi, G. Charlet, and S. Bigo, "Nonlinear effects in mode division multiplexed transmission over few-mode optical fiber," *Photon. Technol. Lett.*, 2012, accepted for publication.

[193] D. Marcuse, A. R. Chraplyvy, and R. W. Tkach, "Effect of fiber nonlinearity on long-distance transmission," *J. Lightw. Technol.*, vol. 9, no. 1, pp. 121–128, Jan. 1991.

[194] R. W. Tkach, A. R. Chraplyvy, F. Forghieri, A. H. Gnauck, and R. M. Derosier, "Four-photon mixing and high-speed WDM systems," *J. Lightw. Technol.*, vol. 13, no. 5, pp. 841–849, May 1995.

[195] G. P. Agrawal, "Modulation instability induced by cross-phase modulation," *Phys. Rev. Lett.*, vol. 59, pp. 880–883, 1987.

[196] M. Yu, C. J. McKinstrie, and G. P. Agrawal, "Instability due to cross-phase modulation in the normal-dispersion regime," *Phys. Rev. E*, vol. 48, no. 3, pp. 2178–2186, 1993.

[197] C. R. Doerr and T. F. Taunay, "Silicon photonics core-, wavelength-, and polarization-diversity receiver," *IEEE Photon. Technol. Lett.*, vol. 23, no. 9, pp. 597–599, May 2011.

ABOUT THE AUTHORS

René-Jean Essiambre (Senior Member, IEEE) received the B.Sc. and Ph.D. degrees in physics and optics, from Université Laval, Québec City, QC, Canada, in 1988 and 1994, respectively. During his Ph.D. studies, he spent one year at McGill University, Montréal, QC, Canada, where he was engaged in research on solid-state physics.

From 1995 to 1997, he was a Postdoctoral Fellow with Prof. Agrawal at The Institute of Optics, University of Rochester, Rochester, NY. Since 1997, he has been at Bell Laboratories, Alcatel-Lucent, Holmdel, NJ. His early research interests includeon optical switching, soliton communication systems, high-power fiber lasers, and mode-locked fiber lasers. His current research interests include high-speed transmission (100 Gb/s and above) and physical layer design of fiber-optic communication systems, including Raman amplification, Rayleigh backscattering, fiber nonlinearities, network design, advanced modulation formats, information theory, and coding. He is the author and coauthor of more than 100 scientific publications and several book chapters. He has served on many conference committees including ECOC, OFC, CLEO, and LEOS. He is program cochair of CLEO: Science and Innovations 2012.

Dr. Essiambre is a Fellow of the Optical Society of America (OSA). He is the recipient of the 2005 OSA Engineering Excellence Award. He is also a Distinguished Member of Technical Staff at Bell Laboratories.

Robert W. Tkach (Fellow, IEEE) received the Ph.D. degree in physics from Cornell University, Ithaca, NY, in 1982.

He is currently the Director of the Advanced Photonics Research Department at Bell Laboratories, Alcatel-Lucent, Crawford Hill, NJ. Prior to rejoining Bell Laboratories in 2006, he was CTO of Celion Networks, Division Manager at AT&T Labs—Research, and a Distinguished Member of Technical Staff at AT&T Bell Laboratories. His research interests include dispersion management, optical amplification, optical networking, and high-speed DWDM transmission systems.

Dr. Tkach was General Cochair of OFC, Vice-President of OIF, Associate Editor of the *Journal of Lightwave Technology* and a member of the IEEE LEOS Board of Governors. He received the Thomas Alva Edison Patent Award from the R&D Council of New Jersey and is a Fellow of the Optical Society of America and AT&T. He received the 2008 John Tyndall Award and in 2009 he was elected to the U.S. National Academy of Engineering and was awarded the 2009 Marconi Prize and Fellowship.